days for the 5 CPs. The mean hospitalization period among IM-like illness patients was 16 ± 4.3 days for APs and 31 ± 9.8 days for CPs.

Clinical presentation following treatment with acyclovir is indicated in Table 5. Bilateral lymphadenopathy symptoms worsened in 13 of the 17 CPs, but dramatically improved in 6 APs ($P = 0.01$). Pharyngeal pain was alleviated in 8 CPs and 6 APs ($P = 0.16$), and headache had subsided in significantly more APs than CPs ($P < 0.01$). Moreover, improvement in arthralgia symptoms was observed in 5 CPs and 6 APs ($P < 0.01$), and mucosal bleeding improved more significantly among APs than CPs ($P < 0.01$). On the other hand, rash was similarly observed in CPs and APs ($P = 0.17$). In general, acyclovir reduced tissue inflammation and symptoms associated with it such as lymphadenopathy, headache, arthralgia, and mucosal bleeding.

Discussion

In this study, we demonstrated the benefits of empirical acyclovir treatment of IM and IM-like illness patients. Acyclovir reduced the duration of hospitalization and of fever; it also led to a rapid decline in the levels of the acute inflammatory marker SAA, within a period of time shorter than the half-life time of ferritin and CRP, which is a chronic inflammation marker. Additionally, acyclovir-mediated improvement in vital signs such as fever, which is indicative of increased inflammatory cytokine secretion as part of the immunological response against the pathogen, was correlated with the laboratory findings. The recovery of neutrophil count was also more prominent than that of lymphocyte count in APs.

The mechanism behind the beneficial effects of acyclovir on AP condition is unknown. One possible explanation is that acyclovir anti-viral activity also inhibits the DNA replication of viruses other than HHV1 to 3. According to a previous study, acyclovir did not exhibit activity against HHV-7 infection (Zhang et al. 1999). On the other hand, acyclovir combined with interferon-beta demonstrated anti-CMV activity in vitro (Spector et al. 1982). Acyclovir antiviral activity against EBV was also reported in vitro (Long et al. 2003). Some studies have shown that acyclovir combined with prednisolone inhibits replication of oropharyngeal EBV without affecting the duration of IM clinical symptoms (Ernberg and Andersson 1986; Tynell et al. 1996). However, no studies have yet reported clinical data indicating that acyclovir is effective in the treatment of EBV-IM and IM-like illness in vivo.

Another possible explanation is that acyclovir exhibits anti-inflammatory activity through suppressing virus-induced cytokine secretion. Studies have reported that HSV enhances the expression of cytokines such as interferon-gamma and tumor necrosis factor-alpha, and that EBV can immortalize B cells activated by cytokines (Wendel-Hansen et al. 1994; Chen et al. 2000). Interestingly, a previous study has reported that acyclovir blocks the expression of inflammatory cytokines (Halford et al. 1997). Moreover, recent reports have shown that antibiotics such as minocycline or macrolides demonstrate anti-inflammatory activity in addition to their known function (Amin et al. 1996).

However, the present study had several disadvantages. For instance, it included a small number of patients, and only clinical features and conventional markers were examined. Therefore, future studies should include a larger number of cases and additional clinical markers such as galectin-9 or osteopontin, which reflect disease activity, should be examined (Chagan-Yasutan et al. 2009; Saitoh et al. 2012).

In conclusion, treatment with acyclovir reduced the duration of hospitalization and of fever without having any evident adverse effects. Therefore, acyclovir treatment may be effective in treating patients suspected of having a viral infection. Additionally, after experiencing a severe earthquake followed by a tsunami in March of 2011 (Shibahara 2011), we observed that, in such resource-limited conditions, acyclovir treatment could constitute one of the initial empirical therapies for IM-like patients.

Acknowledgments

This work was supported by Grant-in-Aid for Scientific Research provided by the Japanese Health, Labor, and Welfare Ministry. This work was also supported by collaborative funding from the Research Center for Zoonosis Control, Hokkaido University, Japan.

Conflict of Interest

The authors state that they have no conflict of interest.

References

Amin, A.R., Attur, M.G., Thakker, G.D., Patel, P.D., Vyas, P.R., Patel, R.N., Patel, I.R. & Abramson, S.B. (1996) A novel mechanism of action of tetracyclines: effects on nitric oxide synthases. *Proc. Natl. Acad. Sci. USA*, **93**, 14014-14019.

Balfour, H.H. Jr., Hokanson, K.M., Schacherer, R.M., Fietzer, C.M., Schmeling, D.O., Holman, C.J., Vezina, H.E. & Brundage, R.C. (2007) A virologic pilot study of valacyclovir in infectious mononucleosis. *J. Clin. Virol.*, **39**, 16-21.

Boeckh, M. (2011) Complications, diagnosis, management, and prevention of CMV infections: current and future. *Hematology Am. Soc. Hematol. Educ. Program*, **2011**, 305-309.

Chagan-Yasutan, H., Saitoh, H., Ashino, Y., Arikawa, T., Hirashima, M., Li, S., Usuzawa, M., Oguma, S., O, Telan, E.F., Obi, C.L. & Hattori, T. (2009) Persistent elevation of plasma osteopontin levels in HIV patients despite highly active antiretroviral therapy. *Tohoku J. Exp. Med.*, **218**, 285-292.

Chen, F.E., Liang, R.H., Lo, J.Y., Yuen, K.Y., Chan, T.K. & Peiris, M. (1997) Treatment of adenovirus-associated hemorrhagic cystitis with ganciclovir. *Bone Marrow Transplant.*, **20**, 997-999.

Chen, S.H., Garber, D.A., Schaffer, P.A., Knipe, D.M. & Coen, D.M. (2000) Persistent elevated expression of cytokine transcripts in ganglia latently infected with herpes simplex virus in the absence of ganglionic replication or reactivation. *Virology*, **278**, 207-216.

Corey, L. (2002) Challenges in genital herpes simplex virus

management. *J. Infect. Dis.*, **186** Suppl. 1, S29-33.
Corey, L. & Wald, A. (2009) Maternal and neonatal herpes simplex virus infections. *N. Engl. J. Med.*, **361**, 1376-1385.
De Clercq, E., Naesens, L., De Bolle, L., Schols, D., Zhang, Y. & Neyts, J. (2001) Antiviral agents active against human herpesviruses HHV-6, HHV-7 and HHV-8. *Rev. Med. Virol.*, **11**, 381-395.
Ernberg, I. & Andersson, J. (1986) Acyclovir efficiently inhibits oropharyngeal excretion of Epstein-Barr virus in patients with acute infectious mononucleosis. *J. Gen. Virol.*, **67**, 2267-2272.
Halford, W.P., Gebhardt, B.M. & Carr, D.J. (1997) Acyclovir blocks cytokine gene expression in trigeminal ganglia latently infected with herpes simplex virus type 1. *Virology*, **238**, 53-63.
Hurt, C. & Tammaro, D. (2007) Diagnostic evaluation of mononucleosis-like illnesses. *Am. J. Med.*, **120**, 911.e1-e8.
Long, M.C., Bidanset, D.J., Williams, S.L., Kushner, N.L. & Kern, E.R. (2003) Determination of antiviral efficacy against lymphotropic herpesviruses utilizing flow cytometry. *Antiviral Res.*, **58**, 149-157.
Luzuriaga, K. & Sullivan, J.L. (2010) Infectious mononucleosis. *N. Engl. J. Med.*, **362**, 1993-2000.
Naito, T., Kudo, N., Inui, A., Matsumoto, N., Takeda, N., Isonuma, H., Dambara, T. & Hayashida, Y. (2006) Causes of infectious mononucleosis-like syndrome in adult patients. *Intern. Med.*, **45**, 833-834.
Prentice, H.G., Gluckman, E., Powles, R.L., Ljungman, P., Milpied, N.F., Rañada, J.M., Mandelli, F., Kho, P., Kennedy, L. & Bell, A.R. (1994) Impact of long-term acyclovir on cytomegalovirus infection and survival after allogeneic bone marrow transplantation. European Acyclovir for CMV Prophylaxis Study Group. *Lancet*, **343**, 749-753.
Rafailidis, P.I., Mavros, M.N., Kapaskelis, A. & Falagas, M.E. (2010) Antiviral treatment for severe EBV infections in apparently immunocompetent patients. *J. Clin. Virol.*, **49**, 151-157.
Rajan, P. & Rivers, J.K. (2001) Varicella zoster virus. Recent advances in management. *Can. Fam. Physician*, **47**, 2299-2304.
Saitoh, H., Ashino, Y., Chagan-Yasutan, H., Niki, T., Hirashima, M. & Hattori, T. (2012) Rapid decrease of plasma galectin-9 levels in patients with acute HIV infection after therapy. *Tohoku J. Exp. Med.*, **228**, 157-161.
Schwetschenau, E. & Kelley, D.J. (2002) The adult neck mass. *Am. Fam. Physician.*, **66**, 831-838.
Shibahara, S. (2011) The 2011 Tohoku earthquake and devastating tsunami. *Tohoku J. Exp. Med.*, **223**, 305-307.
Spector, S.A., Tyndall, M. & Kelley, E. (1982) Effects of acyclovir combined with other antiviral agents on human cytomegalovirus. *Am. J. Med.*, **73**, 36-39.
Torre, D. & Tambini, R. (1999) Acyclovir for treatment of infectious mononucleosis: a meta-analysis. *Scand. J. Infect. Dis.*, **31**, 543-547.
Tynell, E., Aurelius, E., Brandell, A., Julander, I., Wood, M., Yao, Q.Y., Rickinson, A., Akerlund, B. & Andersson, J. (1996) Acyclovir and prednisolone treatment of acute infectious mononucleosis: a multicenter, double-blind, placebo-controlled study. *J. Infect. Dis.*, **174**, 324-331.
Vezina, H.E., Balfour, H.H., Weller, D.R., Anderson, B.J. & Brundage, R.C. (2010) Valacyclovir pharmacokinetics and exploratory pharmacodynamics in young adults with Epstein-Barr virus infectious mononucleosis. *J. Clin. Pharmacol.*, **50**, 734-742.
Vouloumanou, E.K., Rafailidis, P.I. & Falagas, M.E. (2012) Current diagnosis and management of infectious mononucleosis. *Curr. Opin. Hematol.*, **19**, 14-20.
Wendel-Hansen, V., Sällström, J., De Campos-Lima, P.O., Kjellström, G., Sandlund, A., Siegbahn, A., Carlsson, M., Nilsson, K. & Rosén, A. (1994) Epstein-Barr virus (EBV) can immortalize B-cll cells activated by cytokines. *Leukemia*, **8**, 476-484.
Zhang, Y., Schols, D., De Clercq, E. (1999) Selective activity of various antiviral compounds against HHV-7 infection. *Antiviral Res.*, **43**, 23-35.

The International Journal of Biochemistry & Cell Biology 45 (2013) 908–915

Contents lists available at SciVerse ScienceDirect

The International Journal of Biochemistry & Cell Biology

journal homepage: www.elsevier.com/locate/biocel

Mechanism of resistance to S138A substituted enfuvirtide and its application to peptide design

Kazuki Izumi[a], Kumi Kawaji[b], Fusasko Miyamoto[b], Kazuki Shimane[a], Kazuya Shimura[a], Yasuko Sakagami[a], Toshio Hattori[b], Kentaro Watanabe[c], Shinya Oishi[c], Nobutaka Fujii[c], Masao Matsuoka[a], Mitsuo Kaku[d], Stefan G. Sarafianos[e,f], Eiichi N. Kodama[a,b,d,*]

[a] *Laboratory of Virus Control, Institute for Virus Research, Kyoto University, 53 Shogoin Kawaramachi, Sakyo-ku, Kyoto 606-8507, Japan*
[b] *Division of Emerging Infectious Diseases, Tohoku University School of Medicine, Sendai 980-8575, Japan*
[c] *Department of Bioorganic Medical Chemistry, Division of Physical and Organic Chemistry, Graduate School of Pharmaceutical Sciences, Kyoto University, 46-29 Yoshida Shimoadachi-cho, Sakyo-ku, Kyoto 606-8501, Japan*
[d] *Division of Infection Control and Laboratory Diagnostics, Tohoku University School of Medicine, Sendai 980-8575, Japan*
[e] *Christopher S. Bond Life Sciences Center, Department of Molecular Microbiology and Immunology, University of Missouri School of Medicine, Columbia, MO, USA*
[f] *Department of Biochemistry, University of Missouri School of Medicine, Columbia, MO, USA*

ARTICLE INFO

Article history:
Received 31 October 2012
Received in revised form 15 January 2013
Accepted 20 January 2013
Available online 26 January 2013

Keywords:
Resistance
HIV-1
gp41
T-20
Mutation
Fusion inhibitor

ABSTRACT

T-20 (enfuvirtide) resistance is caused by the N43D primary resistance mutation at its presumed binding site at the N-terminal heptad repeat (N-HR) of gp41, accompanied by the S138A secondary mutation at the C-terminal HR of gp41 (C-HR). We have discovered that modifying T-20 to include S138A (T-20_{S138A}) allows it to efficiently block wild-type and T20-resistant viruses, by a mechanism that involves improved binding of T-20_{S138A} to the N-HR that contains the N43D primary mutation. To determine how HIV-1 in turn escapes T-20_{S138A} we used a dose escalation method to select T-20_{S138A}-resistant HIV-1 starting with either wild-type (HIV-1_{WT}) or T-20-resistant (HIV-$1_{N43D/S138A}$) virus. We found that when starting with WT background, I37N and L44M emerged in the N-HR of gp41, and N126K in the C-HR. However, when starting with HIV-$1_{N43D/S138A}$, L33S and I69L emerged in N-HR, and E137K in C-HR. T-20_{S138A}-resistant recombinant HIV-1 showed cross-resistance to other T-20 derivatives, but not to C34 derivatives, suggesting that T-20_{S138A} suppressed HIV-1 replication by a similar mechanism to T-20. Furthermore, E137K enhanced viral replication kinetics and restored binding affinity with N-HR containing N43D, indicating that it acts as a secondary, compensatory mutation. We therefore introduced E137K into T-20_{S138A} (T-$20_{E137K/S138A}$) and revealed that T-$20_{E137K/S138A}$ moderately suppressed replication of T-20_{S138A}-resistant HIV-1. T-$20_{E137K/S138A}$ retained activity to HIV-1 without L33S, which seems to be a key mutation for T-20 derivatives.

Our data demonstrate that secondary mutations can be consistently used for the design of peptide inhibitors that block replication of HIV resistant to fusion inhibitors.

1. Introduction

Human immunodeficiency virus type 1 (HIV-1) fusion to host cell membrane is mediated by formation of a six-helix bundle of the transmembrane subunit gp41 (Chan et al., 1997). Peptides corresponding to amino acid sequences of the gp41 carboxyl-terminal heptad repeat (C-HR) inhibit the HIV-1 fusion by acting as decoys and interfering with the formation of the six-helix bundle (Chan et al., 1998; Malashkevich et al., 1998). Although modified peptides such as SC34EK (Nishikawa et al., 2009), T-2635 (Dwyer et al., 2008), and D-peptides (Welch et al., 2007), and small molecules (Debnath et al., 1999) have been developed, T-20 (enfuvirtide) is the only fusion inhibitor approved for HIV therapy. It is a 36 amino acid peptide derived from the sequence of C-HR of gp41. It is thought to bind at the N-HR domain of gp41 and interfere with the C-HR-N-HR interactions required for membrane fusion and injection of virus into the host cell. T-20 has potent anti-HIV-1 activity and effectively suppresses replication of HIV-1 *in vivo* (Kilby et al., 1998; Lalezari et al., 2003; Lazzarin et al., 2003). However, HIV-1 rapidly develops resistance through mutations in the amino-terminal HR (N-HR) of gp41, especially in the region between L33 and L45, which

* Corresponding author at: Division of Emerging Infectious Diseases, Tohoku University School of Medicine, Sendai 980-8575, Japan. Tel.: +81 22 717 7199; fax: +81 22 717 7199.
E-mail addresses: kodama515@med.tohoku.ac.jp, kodausa21@gmail.com (E.N. Kodama).

1357-2725/$ – see front matter © 2013 Elsevier Ltd. All rights reserved.
http://dx.doi.org/10.1016/j.biocel.2013.01.015

is thought to be the binding site of T-20 (Aquaro et al., 2006; Cardoso et al., 2007; He et al., 2008). Among these residues, N43D in the N-HR is one of the representative mutations for resistance to T-20 (Bai et al., 2008; Cabrera et al., 2006; Oliveira et al., 2009; Izumi et al., 2009; Ueno et al., 2009). Interestingly, most variants show impaired replication fitness, and thus often go on to acquire secondary mutations, such as S138A (Xu et al., 2005), in the C-HR region of gp41 that corresponds to the sequence of T-20. We and others have recently demonstrated that S138A functions as secondary resistance mutation and enhances resistance to T-20 by restoring impaired replication kinetics of T-20-resistant variants that contain primary mutations in the N-HR region, most notably N43D (Izumi et al., 2009; Watabe et al., 2009).

To preempt this escape strategy, we have previously designed a peptide analog of T-20 with the S138A change incorporated in it ($T\text{-}20_{S138A}$; Fig. 1A) and showed that this peptide significantly suppresses replication of T-20-resistant HIV-1 through enhancement of binding affinity to mutated N-HR, such as $N\text{-}HR_{N43D}$ (Izumi et al., 2009). Using circular dichroism (CD) and structural analyses, we also demonstrated that the S138A change provided increased stability to the six-helix bundle (Watabe et al., 2009). In subsequent studies, we validated our approach on another peptide-based fusion inhibitor, C34. In this case, we designed a variant of C34 carrying a secondary escape mutation, N126K, selected for the induction of C34 resistance (Nameki et al., 2005) and also present in HIV-1 isolates from T-20 experienced patients (Baldwin et al., 2004; Cabrera et al., 2006; Svicher et al., 2008). We showed that this C34 variant can effectively inhibit replication of C34-resistant HIV-1. These studies provided the proof of principle that it is possible to design improved peptide-based fusion inhibitors that are efficient against a major mechanism of drug resistance through introduction of resistance-associated mutation(s).

It remains unknown to this date how HIV-1 develops further resistance to $T\text{-}20_{S138A}$. Moreover, it is not known whether we can expand our strategy and modify $T\text{-}20_{S138A}$ to include the secondary mutation(s) that emerge during the selection of $T\text{-}20_{S138A}$-resistant HIV, resulting in a strategy that is applicable to the design of peptides customized to address viral resistance mutations. Hence, in the current study we selected $T\text{-}20_{S138A}$-resistant HIV-1 *in vitro* by a dose-escalating method. We revealed that the resistance mutations that emerged during selection experiments with wild-type or T-20-resistant HIV-1 are located in both the N-HR and the C-HR regions. Furthermore, the I37N and L33S mutations appeared to act as primary mutations for wild-type and T-20-resistant HIV-1, respectively. E137K, a C-HR mutation located in the T-20 sequence, improved replication kinetics and enhanced affinity to N-HR, indicating that E137K acts as a secondary mutation. Introducing the E137K change into the $T\text{-}20_{S138A}$ ($T\text{-}20_{E137K/S138A}$) resulted into a peptide inhibitor effective against $T\text{-}20_{S138A}$-resistant variants, suggesting that secondary or compensatory mutations can be widely applicable to the design of next generation peptide-based inhibitors that are active against HIV-1 resistant to earlier generation fusion-targeting drugs.

2. Materials and methods

2.1. Cells and viruses

MT-2 and 293T cells were grown in RPMI 1640 medium and Dulbecco's modified Eagle medium-based culture medium, respectively. HeLa-CD4-LTR-β-gal cells were kindly provided by Dr. M. Emerman through the AIDS Research and Reference Reagent Program, Division of AIDS, National Institute of Allergy and Infectious Disease (Bethesda, MD), and used for the drug susceptibility assay, as previously described (Nameki et al., 2005; Nishikawa et al., 2009). Recombinant infectious HIV-1 clones carrying various mutations were generated through site-directed mutagenesis of the pNL4-3 plasmid, as previously described (Nameki et al., 2005; Nishikawa et al., 2009). Each molecular clone was transfected into 293T cells with *Trans*IT (Madison, WI). After 48 h, the supernatants were harvested and stored at −80 °C.

2.2. Antiviral agents

The peptides used in this study (Fig. 1A) were chemically synthesized using standard Fmoc-based solid-phase techniques, as previously described (Oishi et al., 2008; Otaka et al., 2002). An HIV-1 reverse transcriptase inhibitor, 2′,3′-dideoxycytidine (ddC) was purchased from Sigma–Aldrich Japan (Tokyo, Japan) and used as a control.

2.3. Determination of drug susceptibility

Peptide sensitivity of infectious clones was determined by the multinuclear activation of galactosidase indicator (MAGI) assay as previously described (Nameki et al., 2005; Nishikawa et al., 2009). Briefly, the target cells (HeLa-CD4-LTR-β-gal; 10^4 cells/well) were plated in flat 96-well microtiter culture plates. On the following day, the cells were inoculated with the HIV-1 clones (60 MAGI units/well, resulting into 60 blue cells after 48 h incubation) and cultured in the presence of various concentrations of drugs in fresh medium. Forty-eight hours after virus exposure, all the blue cells stained with X-gal (5-bromo-4-chloro-3-indolyl-β-D-galactopyranoside) were counted in each well. The activity of test compounds was determined as the concentration that reduced HIV-1 infection by 50% (50% effective concentration [EC_{50}]).

2.4. Induction of HIV-1 variants resistant to $T\text{-}20_{S138A}$

MT-2 cells were exposed to HIV-1 and cultured in the presence of $T\text{-}20_{S138A}$. Cultures were incubated at 37 °C until an extensive cytopathic effect (CPE) was observed. The culture supernatants were used for further passages in MT-2 cells in the presence of two-fold increasing concentrations of $T\text{-}20_{S138A}$ when massive CPEs were seen in the earlier periods. Each passage usually took 5–7 days. The timing is highly dependent on the type of specific mutations introduced, as previously reported (Nameki et al., 2005; Shimura et al., 2010). For example, a passage that follows introduction of novel mutation(s) should shorten the passage period to perhaps 4–5 days. However, there will be longer delays for passages where there are no novel mutations or when there is appearance of only secondary mutations. The dose-escalation process was repeated until resistant variants were obtained. This selection was carried out for a total of 60 passages (approximately 1 year). At the indicated passages (Fig. 1B and C), the sequence of the *env* region was determined by direct sequencing of the proviral DNA extracted from the infected MT-2 cells.

2.5. Viral replication kinetics assay

MT-2 cells (10^5 cells/1 mL) were infected with each virus preparation (500 MAGI units) for 16 h. Infected cells were then washed and cultured in a final volume of 3 mL. The culture supernatants were collected on day 2 through day 5 post-infection, and amounts of p24 antigen were determined.

2.6. CD spectroscopy

Each peptide was incubated at 37 °C for 30 min (the final concentrations of peptides were 10 μM in phosphate buffered saline [PBS];

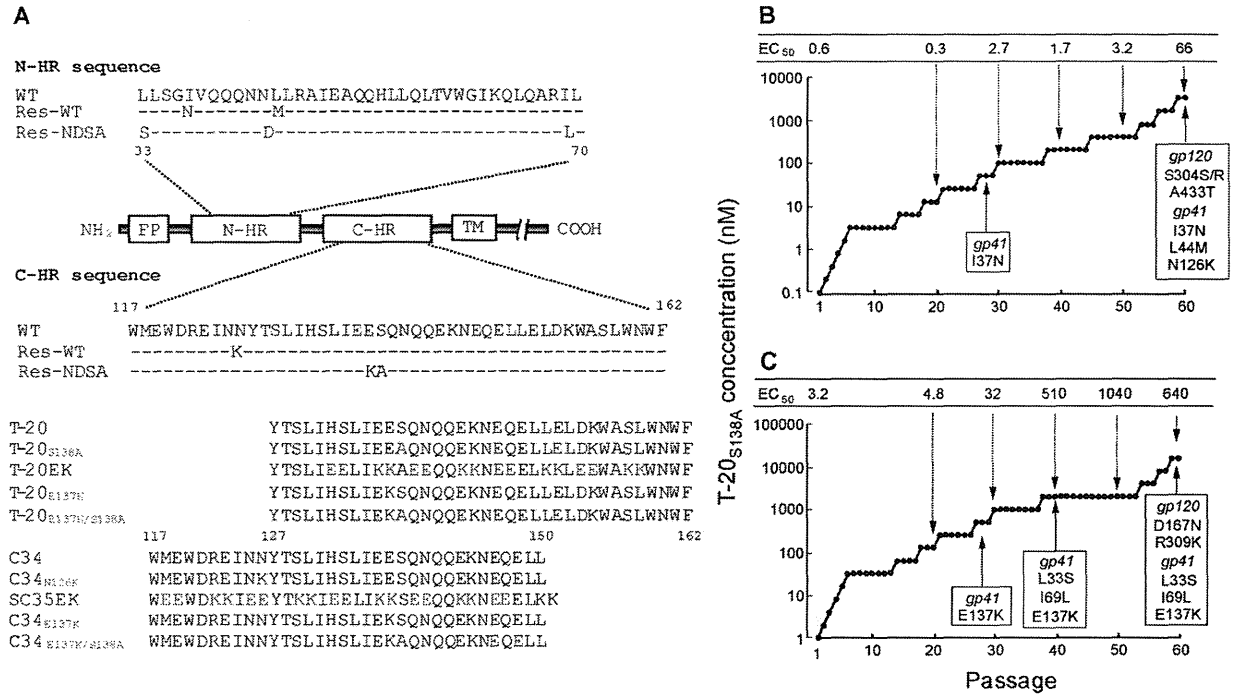

Fig. 1. Domains of gp41 and induction of T-20_{S138A}-resistant HIV-1. (A) Domains of gp41, substitutions observed during *in vitro* passage with T-20_{S138A}, and amino acid sequences of T-20- and C34-based peptides used in this study. The locations of the fusion peptide (FP), amino-terminal heptad region (N-HR), carboxyl-terminal heptad region (C-HR), transmembrane domain (TM), and C-HR-derived peptides are shown. The residue numbers of T-20 and C34 correspond to their positions in gp41. Substitutions of N- and C-HR in gp41 of wild-type (WT) and T-20_{S138A}-resistant HIV-1 are shown. Res.-WT and Res.-NDSA indicate resistant HIV-1 that were initially selected from wild-type and HIV-$1_{N43D/S138A}$, respectively. (B and C) Induction of T-20_{S138A}-resistant HIV-1 by dose-escalating selection in MT-2 cells. Induction of resistant HIV-1 was carried out for a total of 60 passages of HIV-1_{WT} (B) and HIV-$1_{N43D/S138A}$ (C), in 0.1 nM and 1 nM of T-20_{S138A}, respectively. At the indicated passages, proviral DNA was sequenced, and the EC_{50} values of the HIV-1 variants were determined using the MAGI assay. To improve the replication kinetics, substitution of D36G was introduced into the NL4-3 background used in this study (wild-type virus) (Izumi et al., 2009; Mink et al., 2005).

pH 7.4). CD spectra were recorded on an AVIV model 202 spectropolarimeter (Aviv Instruments, Proterion Corporation, Piscataway, NJ) with a 1 mm path-length cuvette at 25 °C as the average of eight scans. The thermal stability was assessed by monitoring the change in the CD signal at 222 nm. The midpoint of the thermal unfolding transition (melting temperature [T_m]) of each complex was determined as previously described (Izumi et al., 2009).

3. Results

3.1. Selection of HIV-1 resistant to T-20_{S138A}

An HIV-1_{NL4-3} strain containing a D36G substitution, which improves replication kinetics, was used as a wild-type virus (HIV-1_{WT}) and for the construction of various mutants, as described (Izumi et al., 2009; Mink et al., 2005). HIV-1_{WT} or T-20-resistant HIV-$1_{N43D/S138A}$ were used for selection of T-20_{S138A}-resistant HIV-1. MT-2 cells were infected with HIV-1_{WT} and HIV-$1_{N43D/S138A}$, and incubated in the presence of T-20_{S138A} at the initial concentrations of 0.1 nM and 1 nM, respectively. At the indicated passages, the sequence of the *env* region was determined by direct sequencing of the proviral DNA extracted from the infected MT-2 cells. During the selection, mutations in the gp41 were observed and are shown in Fig. 1B and C.

In the selection with HIV-1_{WT} (Fig. 1B), at passage 28 (P-28), when T-20_{S138A} concentration was 51.2 nM (P-28, 51.2 nM), isoleucine at position 37 in the gp41 was substituted to asparagine (I37N). At P-60 (3.3 μM), L44M and N126K in the gp41 further emerged. On the other hand, in the selection with T-20-resistant HIV-$1_{N43D/S138A}$ (Fig. 1C), at P-28 (512 nM) and at P-40 (2 μM), E137K in the gp41, and L33S and I69L in the gp41 emerged, respectively. The emergence of the I69L mutation in diverse HIV-1 strains has been previously reported (Eshleman et al., 2007). At P-60, the resistance of selected viruses from HIV-1_{WT} and HIV-$1_{N43D/S138A}$ to T-20_{S138A}, reached approximately 110- and 200-fold, respectively. These results indicate that even though T-20_{S138A} was active against T-20 resistant variants, resistant HIV-1 emerged relatively rapidly compared with the next generation fusion inhibitors, such as SC34EK, which required 120 passages to acquire the resistance (Shimura et al., 2010).

3.2. Susceptibility of T-20_{S138A}-resistant HIV-1 to T-20 and C34 derivatives

To validate our resistance data we used site-directed mutagenesis to prepare recombinant HIV-1 with the T-20_{S138A}-resistance mutations and examined its susceptibility to T-20 and C34 derivatives with MAGI assay (Table 1). We also used as controls the modified α-helix T-20- and C34-peptide inhibitors, T-20EK (Oishi et al., 2008) and SC35EK (Nishikawa et al., 2009; Shimura et al., 2010), respectively, which are more efficient *in vitro* replication inhibitors of T-20-resistant HIV-1 than T-20 or C34. Finally, we also used as a control $C34_{N126K}$, a modified version of C34 that includes the resistance-associated N126K substitution that effectively suppress replication of C34-resistant HIV-1 *in vitro* (Izumi et al., 2009).

Selected mutations I37N and L33S provided various levels of resistance to T-20 and its derivatives, T-20_{S138A} and T-20EK, apparently acting as primary mutations to peptides with a T-20 backbone (Table 1). Other mutations, L44M, I69L, and E137K, which were

Table 1
Antiviral activity of C-HR-derived peptides against gp41 recombinant viruses.

	EC_{50} (nM)					
	T-20	$T\text{-}20_{S138A}$	T-20EK	C34	$C34_{N126K}$	SC35EK
$HIV\text{-}1_{WT}$ [a]	2.4 ± 0.6	0.6 ± 0.1	1.9 ± 0.5	2.1 ± 0.7	1.6 ± 0.5	2.4 ± 0.9
$HIV\text{-}1_{I37N}$	47 ± 6.9 (**20**)	4.3 ± 1.3 (7.2)	21 ± 2.4 (**11**)	3.3 ± 1.1(1.6)	1.9 ± 0.1 (1.2)	1.0 ± 0.4(0.4)
$HIV\text{-}1_{L44M}$	4.1 ± 1.2 (1.7)	0.7 ± 0.2 (1.2)	2.2 ± 0.6 (1.2)	1.1 ± 0.3(0.5)	0.8 ± 0.2 (0.5)	0.6 ± 0.2(0.3)
$HIV\text{-}1_{N126K}$	4.4 ± 1.3 (1.8)	1.2 ± 0.4 (2.0)	2.8 ± 0.2 (1.5)	6.3 ± 1.2(3.0)	1.5 ± 0.2 (0.9)	3.3 ± 0.2(1.4)
$HIV\text{-}1_{I37N/N126K}$	660 ± 180(**275**)	16 ± 4.8 (**27**)	14 ± 5.1 (7.4)	20 ± 4.5(9.5)	3.4 ± 0.4(2.1)	2.9 ± 0.3(1.2)
$HIV\text{-}1_{I37N/L44M/N126K}$	>1000 (>417)	130 ± 40(220)	240 ± 95(126)	66 ± 23 (31)	4.0 ± 0.8 (2.5)	1.1 ± 0.1(0.5)
$HIV\text{-}1_{L33S}$	23 ± 5.5 (9.6)	3.1 ± 0.6 (5.2)	13 ± 2.6 (6.8)	3.2 ± 1.1(1.5)	2.1 ± 0.1 (1.3)	3.0 ± 0.8(1.2)
$HIV\text{-}1_{N43D}$	49 ± 10 (**20**)	3.5 ± 0.9 (5.8)	4.1 ± 1.2 (2.2)	4.4 ± 0.4(2.1)	1.4 ± 0.1 (0.8)	0.4 ± 0.2(0.2)
$HIV\text{-}1_{I69L}$	2.1 ± 0.5 (0.9)	0.5 ± 0.2 (0.8)	2.2 ± 0.4 (1.2)	2.7 ± 0.2(1.3)	2.2 ± 0.5 (1.4)	2.7 ± 0.5(1.1)
$HIV\text{-}1_{E137K}$	2.0 ± 0.3 (0.8)	0.7 ± 0.1 (1.2)	2.5 ± 0.4 (1.3)	2.6 ± 0.2(1.2)	2.3 ± 0.7 (1.4)	3.1 ± 0.8(1.3)
$HIV\text{-}1_{N43D/S138A}$	84 ± 16 (**35**)	3.2 ± 1.0 (5.3)	3.4 ± 1.1 (1.8)	2.7 ± 0.2(1.3)	1.6 ± 0.5 (1.0)	0.3 ± 0.1(0.1)
$HIV\text{-}1_{L33S/N43D/S138A}$	>1000 (**>417**)	550 ± 72(**174**)	330 ± 94 (14)	30 ± 9.2(2.6)	4.2 ± 1.2 (0.4)	0.9 ± 0.3(0.4)
$HIV\text{-}1_{N43D/E137K/S138A}$	110 ± 31 (**46**)	14 ± 4.7 (**23**)	7.0 ± 2.4 (3.7)	7.4 ± 1.9(3.5)	2.1 ± 0.7 (1.3)	1.9 ± 0.6(0.8)
$HIV\text{-}1_{L33S/N43D/E137K/S138A}$	>1000 (**>417**)	>1000(**>1667**)	>1000 (**>526**)	31 ± 5.0 (**15**)	6.7 ± 1.7 (4.2)	1.2 ± 0.2(0.5)
$HIV\text{-}1_{L33S/N43D/I69L/E137K/S138A}$	>1000 (**>417**)	>1000(**>1667**)	>1000 (**>526**)	50 ± 12 (**24**)	28 ± 7.1(**17.5**)	1.0 ± 0.9(0.4)

Anti-HIV activity was determined using the MAGI assay. Fifty percent effective concentration (EC_{50}) values and SD were obtained from the results of at least three independent experiments. Shown in parentheses are the fold-increases in resistance (increase in EC_{50} value) calculated by comparison to a wild-type virus ($HIV\text{-}1_{WT}$). Increases of over 10-fold are indicated in bold.

[a] To improve the replication kinetics, substitution of D36G, observed in majority of HIV-1 strains, was introduced into the NL4-3 background used in this study (wild-type virus; $HIV\text{-}1_{WT}$) (Izumi et al., 2009; Mink et al., 2005).

observed in wild-type HIV-1 as polymorphisms (Kuiken et al., 2010; Loutfy et al., 2007), conferred little resistance to all peptide fusion inhibitors tested. However, introduction of L44M to $HIV\text{-}1_{I37N/N126K}$ ($HIV\text{-}1_{I37N/L44M/N126K}$) remarkably enhanced resistance to T-20 derivatives. This was consistent with previous studies that also reported a resistance enhancement (1.8-fold) by L44M to T-20 (Loutfy et al., 2007). Collectively, these data suggest that L44M has as a role in HIV-1 resistance as a secondary mutation. All peptides sufficiently suppressed $HIV\text{-}1_{I69L}$, suggesting that I69L may be a secondary mutation or a polymorphism. N126K conferred only marginal resistance (<3-fold) to all peptide fusion inhibitors, but in the background of I37N ($HIV\text{-}1_{I37N/N126K}$) it enhanced resistance to T-20, $T\text{-}20_{S138A}$, and C34. L33S, which was originally reported as a C34 resistance associated mutation (Armand-Ugon et al., 2003), significantly enhanced resistance in the background of N43D/S138A mutations ($HIV\text{-}1_{L33S/N43D/S138A}$). Similar to the N126K mutation, E137K also enhanced resistance by N43D/S138A ($HIV\text{-}1_{N43D/E137K/S138A}$) and L33S/N43D/S138A ($HIV\text{-}1_{L33S/N43D/E137K/S138A}$) to $T\text{-}20_{S138A}$, T-20, and T-20EK. These results indicate that L33S and I37N appear to be primary mutations for T-20 derivatives.

3.3. *Effect of substitutions in the gp120 on peptide susceptibility*

Polymorphisms in the gp120 that influence co-receptor usage may influence T-20 susceptibility (Labrosse et al., 2003; Reeves et al., 2002). Meanwhile, others reported that T-20 susceptibility was not influenced by co-receptor usage (Cilliers et al., 2004; Melby et al., 2006). Resistance induction experiments performed in this study revealed that most laboratory strains with *in vitro* resistance to fusion inhibitors acquired substitutions in both the gp120 and the gp41 (Armand-Ugon et al., 2003; Eggink et al., 2011; Fikkert et al., 2002; Izumi et al., 2010; Nameki et al., 2005; Shimura et al., 2010). However, most substitutions showed little impact on resistance, and only contributed to a small enhancement of replication capacity (Eggink et al., 2011; Izumi et al., 2010; Nameki et al., 2005; Shimura et al., 2010). In the present study, we examined peptide susceptibility of cloned viruses that contain all Env substitutions observed in the selection (both gp120 and gp41). Most substitutions in the gp120 attenuated resistance to fusion inhibitors (Table 3). Therefore, *in vitro* experiments showed that substitutions in the gp120 are not likely associated with resistance.

3.4. *Influence of mutations in the gp41 on HIV-1 replication*

To address the effects of mutations on HIV-1 replication, we examined the replication kinetics of $T\text{-}20_{S138A}$-resistant $HIV\text{-}1_{N43D/S138A}$ variants. Consistent with a previous report (Lohrengel et al., 2005), the L33S mutation did not significantly affect the replication kinetics and infectivity compared with those of $HIV\text{-}1_{WT}$ (Fig. 2A). The S138A mutation restored the replication

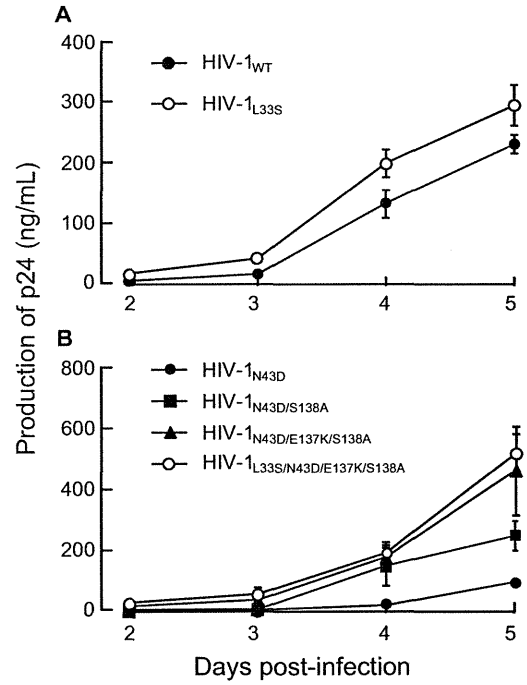

Fig. 2. Replication kinetics of $T\text{-}20_{S138A}$-resistant variants. Replication kinetics of $T\text{-}20_{S138A}$-resistant recombinant variants that introduced L33S mutation (A), or combinations of L33S, E137K, and S138A mutations in $HIV\text{-}1_{N43D}$ (B). To improve replication kinetics, the D36G polymorphism was introduced into the NL4-3 background used in this study ($HIV\text{-}1_{WT}$). Supernatants from infected MT-2 cells were collected on days 2–7 and the amount of p24 produced was determined. Representative results are shown as mean values with standard deviations estimated from three independent experiments.

kinetics of HIV-1_{N43D} (Fig. 2B), as previously described (Izumi et al., 2009). E137K was also associated with N43D mutation *in vivo* (Svicher et al., 2008), and restored infectivity impaired by N43D (Tolstrup et al., 2007). Introduction of E137K into N43D/S138A enhanced the replication kinetics, and further addition of L33S to N43D/E137K/S138A resulted in equivalent replication kinetics compared with HIV-$1_{N43D/E137K/S138A}$ (Fig. 2B) as observed in HIV-1_{WT} based mutants. During the passage of HIV-$1_{N43D/S138A}$, a synonymous mutation at amino acid position L44, TTG to CTG, was observed. Interestingly, $L_{TTG}44L_{CTG}$ enhanced viral replication kinetics through enhanced stability of the Rev-responsive element (RRE) secondary structure (Ueno et al., 2009). Therefore, we examined the viral replication kinetics of mutants with $L_{TTG}44L_{CTG}$, and compared HIV-1_{WT}, with HIV-$1_{L44L\text{-}CTG}$, and HIV-$1_{L33S/N43D/L44L\text{-}CTG/E137K/S138A}$ with HIV-$1_{L33S/N43D/L44L\text{-}CTG/I69L/E137K/S138A}$. As expected, the presence of $L_{TTG}44L_{CTG}$ enhanced replication in all viruses. Surprisingly, mutants with resistance mutations showed enhanced replication kinetics as determined by the p24 production assay of culture supernatants (Fig. 4A). Therefore, we further examined infectivity using the MAGI assay and determined that the infectivity of resistance variants containing $L_{TTG}44L_{CTG}$ was reduced compared with HIV-1_{WT} (Fig. 4B). These results indicate that the primary mutation, L33S, possesses less ability to attenuate HIV-1 replication, while I69L, S138A, and E137K enhance replication kinetics of T-20-resistant HIV-1 to a comparable level of HIV-1_{WT}.

3.5. Circular dichroism

To clarify the effect of E137K substitutions on peptide binding, we examined the binding affinities of E137K-containing C-HR peptides to N-HR using CD analysis. CD spectra reveal the presence of stable α-helical structures of six-helix bundles that are required for biological activity and are thought to mechanistically and thermodynamically correlate with HIV-1 fusion (Bianchi et al., 2005). Since *in vitro* T-20 does not interact with the N36 peptide (amino acid positions 35–70 of the N-HR), we used instead peptide C34 with E137K and/or S138A substitutions (Fig. 1A). We found that mixtures of $C34_{E137K}$, $C34_{S138A}$, or $C34_{E137K/S138A}$ with N36 or $N36_{N43D}$ showed sufficient and comparable α-helicity at 25 °C (Fig. 3A and B). We also determined the thermal stability of the helical complexes formed by the N36 and C34 peptides, which is also an indication of the binding affinity of these peptides. Hence, we measured and compared the melting temperatures (T_m) of various complexes, which indicates the 50% disruption of the six-helix bundle (Fig. 3C). Complexes of N36 and C34 containing the S138A and E137K/S138A substitutions (N36/$C34_{S138A}$ and N36/$C34_{E137K/S138A}$, respectively), showed higher thermal stability than N36/C34. Similarly, S138A and E137K/S138A restored the binding affinity of C34 to $N36_{N43D}$. These results indicate that E137K acts as a compensatory mutation for the T-20_{S138A}-resistance primary mutation, causing enhancement of replication kinetics.

3.6. Antiviral activity of E137K-modified peptides

Recently, we demonstrated that introduction of the S138A secondary mutation to T-20 (T-20_{S138A}) enhanced binding to mutated N-HR and suppresses resistance of T-20-resistance variants (Izumi et al., 2009). Similarly, as shown in Fig. 3, E137K enhanced binding affinity with N-HR, suggesting that introduction of E137K to T-20 may enhance the antiviral activity of T-20. We synthesized T-20 and T-20_{S138A} variants containing the E137K change (T-20_{E137K} and T-$20_{E137K/S138A}$) (Fig. 1A) and examined their anti-HIV activity against T-20_{S138A}-resistant HIV-1 (Table 2). All peptides exhibited potent antiviral activity against HIV-1_{WT}. HIV-$1_{L33S/N43D/S138A}$ and HIV-$1_{I37N/L44M/N126K}$ showed high resistance to T-20_{E137K},

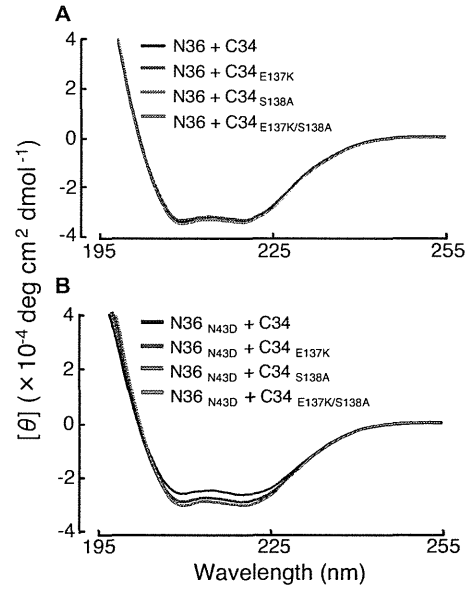

C

	T_m (°C)	
	N36	$N36_{N43D}$
C34	67.6	53.2
$C34_{E137K}$	68.9	56.7
$C34_{S138A}$	73.2	58.0
$C34_{E137K/S138A}$	74.6	63.3

Fig. 3. CD spectra (A and B) and thermal stability (C) of N36/C34 complexes. Peptide sequences used in this study are shown in FIG 1A and have also been previously described (Izumi et al., 2009). CD spectra of $C34_{E137K}$, $C34_{S138A}$, and $C34_{E137K/S138A}$ complexes with N36 (A) and $N36_{N43D}$ (B) are shown. Equimolar amounts (10 μM) of the N- and C-HR peptides were incubated at 37 °C for 30 min in PBS. The CD spectra of each mixture were then collected at 25 °C using a Jasco (Model J-710) spectropolarimeter. (C) Thermal stabilities, defined as the midpoint of the thermal unfolding transition (T_m) values, of the potential six-helix bundles of N- and C-HR peptides, were determined.

indicating that the resistance mechanism of T-20_{E137K} is similar to that of T-20_{S138A}. On the other hand, T-$20_{E137K/S138A}$ (Table 2) maintained some antiviral activity against HIV-$1_{L33S/N43D/S138A}$, HIV-$1_{L33S/N43D/E137K/S138A}$, and HIV-$1_{I37N/L44M/N126K}$ compared with other T-20 derivatives including electrostatically constrained T-20EK (Table 1 and Fig. 1). $C34_{E137K}$ and $C34_{E137K/S138A}$ significantly suppressed all HIV-1 variants tested except for HIV-$1_{I37N/L44M/N126K}$ by $C34_{E137K}$. These results indicate that peptides with resistant mutations may sustain their activity against particular resistant variants.

4. Discussion

The current study describes the introduction of resistance changes into the original and modified (T-20_{S138A}) versions of the T-20 peptide-fusion inhibitor. We analyzed the new T-20 derivatives using both wild-type and T-20-resistant strains. We also identified through dose escalation experiments, T-20_{S138A}-resistants. We found that T-20_{S138A}-resistant HIV-1 showed cross-resistance only to the T-20 derivatives, but not to C34 derivatives. Through the CD analysis, the N126K and E137K mutations in the C-HR may act as compensatory mutations for impaired interaction by a primary mutation, I37N and N43D in the N-HR, respectively. Since E137K is located within the T-20 sequence, we synthesized and characterized the activity of novel T-20-based peptides containing E137K (T-20_{E137K}). Here we demonstrate that

Table 2
Antiviral activity of E137K-induced C-HR peptides against T-20_{S138A}-resistant variants.

	EC_{50} (nM)			
	T-20_{E137K}	T-$20_{E137K/S138A}$	$C34_{E137K}$	$C34_{E137K/S138A}$
HIV-1_{WT} [a]	0.8 ± 0.2	0.5 ± 0.1	1.0 ± 0.3	0.7 ± 0.2
HIV-1_{L33S}	13 ± 3.2 (**16**)	2.2 ± 0.4 (4.5)	0.7 ± 0.2(0.7)	0.5 ± 0.1(0.7)
HIV-$1_{N43D/S138A}$	4.2 ± 0.7 (5.3)	0.7 ± 0.2 (1.4)	0.3 ± 0.1(0.3)	0.4 ± 0.1(0.6)
HIV-$1_{L33S/N43D/S138A}$	700 ± 150 (**880**)	45 ± 9.9 (**90**)	2.3 ± 0.4(2.3)	0.5 ± 0.2(0.7)
HIV-$1_{N43D/E137K/S138A}$	12 ± 3.6 (**15**)	2.4 ± 0.8 (4.8)	0.2 ± 0.1(0.2)	0.4 ± 0.1(0.6)
HIV-$1_{L33S/N43D/E137K/S138A}$	480 ± 47 (**600**)	36 ± 3.1 (**72**)	3.8 ± 1.3(3.8)	1.0 ± 0.4(1.4)
HIV-$1_{L33S/N43D/I69L/E137K/S138A}$	1808 ± 852(2260)	157 ± 83(314)	4 ± 2 (4)	1.0 ± 0.4(1.4)
HIV-$1_{I37N/L44M/N126K}$	200 ± 24 (**250**)	30 ± 8.7 (**60**)	17 ± 3.8 (**17**)	2.2 ± 0.3(3.1)

Anti-HIV activity was determined using the MAGI assay. Fifty percent effective concentration (EC_{50}) values and SD were obtained from the results of at least three independent experiments. Shown in parentheses are the fold-increases in resistance (increase in EC_{50} value) calculated by comparison to a wild-type virus (HIV-1_{WT}). Increases of over 10-fold are indicated in bold.

[a] To improve the replication kinetics, substitution of D36G, observed in majority of HIV-1 strains, was introduced into the NL4-3 background used in this study (wild-type virus; HIV-1_{WT}) (Izumi et al., 2009; Mink et al., 2005).

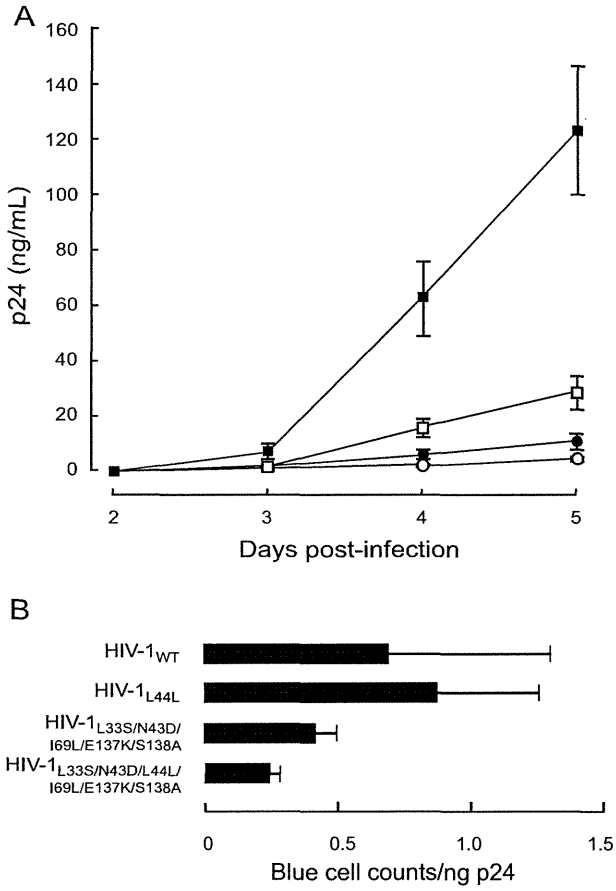

Fig. 4. Effect of secondary mutations in the N-HR on (A) replication kinetics and (B) infectivity. $L_{TTG}44L_{CTG}$ was introduced into HIV-1_{WT} and T-20_{S138A} resistant HIV-1 (HIV-$1_{L33S/N43D/L44L\text{-}CTG/I69L/E137K/S138A}$). Replication kinetics were determined by measuring p24 production in culture supernatants. HIV-1_{WT} (open circles), HIV-1_{L44L} (closed circles) HIV-$1_{L33S/N43D/I69L/E137K/S138A}$ (open squares), and HIV-$1_{L33S/N43D/L44L\text{-}CTG/I69L/E137K/S138A}$ (closed squares). $L_{TTG}44L_{CTG}$ introduction statistically enhanced both replication of HIV-1_{WT} and HIV-$1_{L33S/N43D/L44L\text{-}CTG/I69L/E137K/S138A}$ (Student's *t*-test, $p < 0.01$ on day 4 and 5). Relative infectivity (blue cell counts in MAGI cells divided by amount of p24) was calculated (B). Error bars indicate SD of three determinations. Decrease of infectivity between HIV-$1_{L33S/N43D/I69L/E137K/S138A}$ and HIV-$1_{L33S/N43D/L44L\text{-}CTG/I69L/E137K/S138A}$ were statistically significant (Student's *t*-test, $p < 0.05$).

the introduction of a secondary resistance mutation (E137K) in the backbone of a peptide fusion inhibitor is a useful change that results into more potent fusion inhibitors, even for HIV-1 strains that are resistant to peptide fusion inhibitors.

Selection of T-20_{S138A}-resistance starting with wild-type HIV-1 resulted in the emergence of I37N and L44M substitutions, which were located in the N-HR region that is thought to interact with T-20. Other substitutions at position 37 (I37T or I37K) also conferred resistance to T-20 and C34 (Nameki et al., 2005), suggesting that I37 in N-HR is critical for the attachment of C-HR-derived peptide fusion inhibitors. The L44M mutation has only been observed in subtype B HIV-1-infected patients treated with T-20 (Carmona et al., 2005), and conferred weak resistance to T-20 (Loutfy et al., 2007). In this study, L44M did not confer resistance to all peptide inhibitors; however, L44M in combination with other mutations (I37N/N126K) remarkably enhanced resistance to T-20_{S138A}, suggesting that L44M serves as a secondary mutation to enhance resistance to T-20_{S138A}. N126K also enhances resistance to some fusion inhibitors (Baldwin et al., 2004; Nameki et al., 2005; Eggink et al., 2008) by helping recover losses in intra-gp41 interactions that were caused by primary mutations, such as N43D.

When we selected T-20_{S138A}-resistant HIV-1 (HIV-$1_{N43D/S138A}$) we obtained a somehow different set of mutations that included L33S, which is located at the presumed T-20 binding site at N-HR, as well as I37N, N43D, and L44M. L33S was previously reported in HIV-1 variants resistant to T-20 (Fikkert et al., 2002), C34 (Armand-Ugon

Table 3
Antiviral activity of C-HR-derived peptides against gp160 recombinant viruses.

Compound	EC_{50} (nM)	
ddC	771 ± 272	
T-20 derivatives		
T20	>10,000	(NA)
T20EK	2729 ± 1113	(NA)
$T20_{S138A}$	3126 ± 453	(NA)
$T20_{E137K}$	2761 ± 1477	(NA)
$T20_{E137K/S138A}$	203 ± 54	(0.6)
C34 derivatives		
C34	171.0 ± 106	(3.4)
$C34_{N126K}$	25.9 ± 4.6	(NA)
SC34EK	1.0 ± 0.8	(1)
$C34_{E137K}$	7.0 ± 4.4	(0.4)
$C34_{E137K/S138A}$	0.3 ± 0.1	(0.3)

Anti-HIV activity was determined using the MAGI assay. Fifty percent effective concentration (EC_{50}) values and SD were obtained from the results of at least three independent experiments. Shown in parentheses are the fold-increases in resistance (increase in EC_{50} value) calculated by comparison to the resistant clone with mutations only in gp41 (HIV-$1_{L33S/N43D/I69L/E137K/S138A}$). To improve the replication kinetics, substitution of D36G, observed in majority of HIV-1 strains, was introduced into the NL4-3 background used in this study (Izumi et al., 2009; Mink et al., 2005). NA, not available; ddC, dideoxycytidine.

et al., 2003), and a membrane-anchored C-HR-derived peptide, M87 (Lohrengel et al., 2005). Although our work clearly demonstrates that L33S is involved in resistance to T-20 derivatives, it was not possible to discern whether L33S affected binding affinity to C-HR in the CD analyses because L33 was not in the sequence of the N36 N-HR peptide that we had to use in this study. As shown in Fig. 2, L33S did not significantly affect replication kinetics compared with HIV-1_{WT}, suggesting that L33S might sustain binding affinity with C-HR to form a stable six-helix bundle. The L33S mutation is located in the loop of stem IIc of the RRE (Ueno et al., 2009). Hence, nucleotide changes for L33S do not require compensatory mutations to maintain secondary structure of the RRE. Therefore, it is likely that L33S has little effect on replication kinetics. In this study, L33S conferred little resistance to C34 in this study, while it was previously reported to confer up to 10-fold resistance (Armand-Ugon et al., 2003), suggesting that some other viral background might affect the resistance, since Armand-Ugon et al. (2003) examined bulk virus samples obtained from the selection.

A prevalent polymorphism, E137K, which was associated with N43D *in vivo* (Svicher et al., 2008), has been proven to restore infectivity that has been impaired by N43D (Tolstrup et al., 2007). E137K did not affect susceptibility to all peptide fusion inhibitors by itself, but in combination with primary mutations, it remarkably enhanced resistance to T-20_{S138A}. Moreover, introduction of the E137K change into N43D/S138A enhanced the viral replication kinetics as shown in Fig. 2. A possible hydrogen bond between K137 and D43 may partially restore the reported loss in six-helix bundle stability conferred by the N43D mutation (Bai et al., 2008), suggesting that E137K can compensate for losses in the interactions between N-HR_{N43D} and C-HR. This hypothesis is consistent with our CD results presented in Fig. 3.

Because E137K restored binding affinity with N-HR similar to the S138A mutation, we expected that introduction of E137K into T-20 would effectively suppresses replication of T-20-resistant HIV-1. We examined the antiviral activity of E137K- and E137K/S138A-containing T-20 and C34 to T-20_{S138A}-resistant HIV-1. We found that T-20_{E137K} had similar antiviral activity with other T-20 derivatives such as T-20_{S138A} and T-$20_{E137K/S138A}$. Hence, we believe that the combination of few substitution secondary mutations can enhance the antiviral activity of peptide fusion inhibitors. Therefore, it is possible to design peptides that include the secondary mutations in the C-HR and use them by themselves and/or in combinations to block fusion inhibitor resistant viruses. Importantly, we have successfully applied this strategy to suppress HIV-1 resistance to next generation fusion inhibitor SC34EK (Shimura et al., 2010).

In this study, we identified two distinct pathways to escape pressure of T-20_{S138A}. Emergence of drug resistance mutants under drug pressure involves a stochastic selection. Nonetheless, the makeup of the final population depends on both the ability of specific populations to evade the drug, as well as their fitness that determines their representation in the escape population. There are several examples in the literature where HIV becomes resistant to the same drug by different mechanisms. For example, in the case of the most commonly used drugs that target HIV reverse transcriptase (RT), the virus can develop multidrug resistance by either the Q151M complex pathway (Kavlick et al., 1998; Shirasaka et al., 1995) or by accumulation of thymidine associated mutations (TAMs) (Hachiya et al., 2008; Kosalaraksa et al., 1999). We recently report some of background polymorphisms can also influence resistance pathways, such 172R/K in the RT region (Hachiya et al., 2012). In the case of the T-20S138A inhibitor, the N43D/S138A may also act as such polymorphisms despite the presence of primary mutations (Izumi et al., 2009) and preferentially affect the emergence of specific mutations.

5. Conclusion

As previously discussed (Izumi et al., 2009), although other developed peptide-based fusion inhibitors need many amino acid additions and/or substitutions for the enhancement of their antiviral activity (Chinnadurai et al., 2007; Eggink et al., 2008; Dwyer et al., 2007; Otaka et al., 2002), application of secondary mutations similar to T-20_{S138A} and T-$20_{E137K/S138A}$ is straightforward. It is based on information from viral evolution studies under drug pressure that help design improved inhibitors.

Acknowledgments

This work was supported by a grant from the Ministry of Education, Culture, Sports, Science, and Technology of Japan, a grant for the Promotion of AIDS Research from the Ministry of Health, Labour and Welfare. Additional support was by National Institute of Health (NIH) research Grants AI094715, AI076119, AI079801, and AI100890 (SGS). We are grateful to Biomedical Research Core (Tohoku University School of Medicine) for technical support. The authors declare non-financial competing interests.

References

Aquaro S, D'Arrigo R, Svicher V, Perri GD, Caputo SL, Visco-Comandini U, et al. Specific mutations in HIV-1 gp41 are associated with immunological success in HIV-1-infected patients receiving enfuvirtide treatment. Journal of Antimicrobial Chemotherapy 2006;58:714–22.

Armand-Ugon M, Gutierrez A, Clotet B, Este JA. HIV-1 resistance to the gp41-dependent fusion inhibitor C-34. Antiviral Research 2003;59:137–42.

Bai X, Wilson KL, Seedorff JE, Ahrens D, Green J, Davison DK, et al. Impact of the enfuvirtide resistance mutation N43D and the associated baseline polymorphism E137K on peptide sensitivity and six-helix bundle structure. Biochemistry 2008;47:6662–70.

Baldwin CE, Sanders RW, Deng Y, Jurriaans S, Lange JM, Lu M, et al. Emergence of a drug-dependent human immunodeficiency virus type 1 variant during therapy with the T20 fusion inhibitor. Journal of Virology 2004;78:12428–37.

Bianchi E, Finotto M, Ingallinella P, Hrin R, Carella AV, Hou XS, et al. Covalent stabilization of coiled coils of the HIV gp41N region yields extremely potent and broad inhibitors of viral infection. Proceedings of the National Academy of Sciences of the United States of America 2005;102:12903–8.

Cabrera C, Marfil S, Garcia E, Martinez-Picado J, Bonjoch A, Bofill M, et al. Genetic evolution of gp41 reveals a highly exclusive relationship between codons 36, 38 and 43 in gp41 under long-term enfuvirtide-containing salvage regimen. AIDS 2006;20:2075–80.

Cardoso RM, Brunel FM, Ferguson S, Zwick M, Burton DR, Dawson PE, et al. Structural basis of enhanced binding of extended and helically constrained peptide epitopes of the broadly neutralizing HIV-1 antibody 4E10. Journal of Molecular Biology 2007;365:1533–44.

Carmona R, Perez-Alvarez L, Munoz M, Casado G, Delgado E, Sierra M, et al. Natural resistance-associated mutations to enfuvirtide (T20) and polymorphisms in the gp41 region of different HIV-1 genetic forms from T20 naive patients. Journal of Clinical Virology 2005;32:248–53.

Chan DC, Chutkowski CT, Kim PS. Evidence that a prominent cavity in the coiled coil of HIV type 1 gp41 is an attractive drug target. Proceedings of the National Academy of Sciences of the United States of America 1998;95:15613–7.

Chan DC, Fass D, Berger JM, Kim PS. Core structure of gp41 from the HIV envelope glycoprotein. Cell 1997;89:263–73.

Chinnadurai R, Rajan D, Munch J, Kirchhoff F. Human immunodeficiency virus type 1 variants resistant to first- and second-version fusion inhibitors and cytopathic in ex vivo human lymphoid tissue. Journal of Virology 2007;81:6563–72.

Cilliers T, Patience T, Pillay C, Papathanasopoulos M, Morris L. Sensitivity of HIV type 1 subtype C isolates to the entry inhibitor T-20. AIDS Research and Human Retroviruses 2004;20:477–82.

Debnath AK, Radigan L, Jiang S. Structure-based identification of small molecule antiviral compounds targeted to the gp41 core structure of the human immunodeficiency virus type 1. Journal of Medicinal Chemistry 1999;42:3203–9.

Dwyer JJ, Wilson KL, Davison DK, Freel SA, Seedorff JE, Wring SA, et al. Design of helical, oligomeric HIV-1 fusion inhibitor peptides with potent activity against enfuvirtide-resistant virus. Proceedings of the National Academy of Sciences of the United States of America 2007;104:12772–7.

Dwyer JJ, Wilson KL, Martin K, Seedorff JE, Hasan A, Medinas RJ, et al. Design of an engineered N-terminal HIV-1 gp41 trimer with enhanced stability and potency. Protein Science 2008;17:633–43.

Eggink D, Baldwin CE, Deng Y, Langedijk JP, Lu M, Sanders RW, et al. Selection of T1249-resistant human immunodeficiency virus type 1 variants. Journal of Virology 2008;82:6678–88.

Eggink D, Bontjer I, Langedijk JP, Berkhout B, Sanders RW. Resistance of human immunodeficiency virus type 1 to a third-generation fusion inhibitor requires

multiple mutations in gp41 and is accompanied by a dramatic loss of gp41 function. Journal of Virology 2011;85:10785–97.
Eshleman SH, Hudelson SE, Bruce R, Lee T, Owens MR, Hackett J, et al. Analysis of HIV type 1 gp41 sequences in diverse HIV type 1 strains. AIDS Research and Human Retroviruses 2007;23:1593–8.
Fikkert V, Cherepanov P, Van Laethem K, Hantson A, Van Remoortel B, Pannecouque C, et al. env chimeric virus technology for evaluating human immunodeficiency virus susceptibility to entry inhibitors. Antimicrobial Agents and Chemotherapy 2002;46:3954–62.
Hachiya A, Kodama EN, Sarafianos SG, Schuckmann MM, Sakagami Y, Matsuoka M, Takiguchi M, Gatanaga H, Oka S. Amino acid mutation N348I in the connection subdomain of human immunodeficiency virus type 1 reverse transcriptase confers multiclass resistance to nucleoside and nonnucleoside reverse transcriptase inhibitors. Jouranl of Virology 2008;82:3261–70.
Hachiya A, Marchand B, Kirby KA, Michailidis E, Tu X, Palczewski K, Ong YT, Li Z, Griffin DT, Schuckmann MM, Tanuma J, Oka S, Singh K, Kodama EN, Sarafianos SG. HIV-1 reverse transcriptase (RT) polymorphism 172K suppresses the effect of clinically relevant drug resistance mutations to both nucleoside and non-nucleoside RT inhibitors. Journal of Biological Chemistry 2012;287:29988–99.
He Y, Xiao Y, Song H, Liang Q, Ju D, Chen X, et al. Design and evaluation of sifuvirtide, a novel HIV-1 fusion inhibitor. Journal of Biological Chemistry 2008;283:11126–34.
Izumi K, Kodama E, Shimura K, Sakagami Y, Watanabe K, Ito S, et al. Design of peptide-based inhibitors for human immunodeficiency virus type 1 strains resistant to T-20. Journal of Biological Chemistry 2009;284:4914–20.
Izumi K, Nakamura S, Nakano H, Shimura K, Sakagami Y, Oishi S, et al. Characterization of HIV-1 resistance to a fusion inhibitor, N36, derived from the gp41 amino-terminal heptad repeat. Antiviral Research 2010;87:179–86.
Kavlick MF, Wyvill K, Yarchoan R, Mitsuya H. Emergence of multidideoxynucleoside-resistant human immunodeficiency virus type 1 variants, viral sequence variation, and disease progression in patients receiving antiretroviral chemotherapy. Journal of Infectious Diseases 1998;177:1506–13.
Kilby JM, Hopkins S, Venetta TM, DiMassimo B, Cloud GA, Lee JY, et al. Potent suppression of HIV-1 replication in humans by T-20, a peptide inhibitor of gp41-mediated virus entry. Nature Medicine 1998;4:1302–7.
Kosalaraksa P, Kavlick MF, Maroun V, Le R, Mitsuya H. Comparative fitness of multi-dideoxynucleoside-resistant human immunodeficiency virus type 1 (HIV-1) in an In vitro competitive HIV-1 replication assay. Jouranl of Virology 1999;73:5356–63.
Kuiken C, Foley B, Leitner T, Apetrei C, Hahn B, Mizrachi I, et al. HIV sequence compendium 2010. Los Alamos, NM: Los Alamos National Laboratory, Theoretical Biology and Biophysics; 2010.
Labrosse B, Labernardiere JL, Dam E, Trouplin V, Skrabal K, Clavel F, et al. Baseline susceptibility of primary human immunodeficiency virus type 1 to entry inhibitors. Journal of Virology 2003;77:1610–3.
Lalezari JP, Henry K, O'Hearn M, Montaner JS, Piliero PJ, Trottier B, et al. Enfuvirtide, an HIV-1 fusion inhibitor, for drug-resistant HIV infection in North and South America. New England Journal of Medicine 2003;348:2175–85.
Lazzarin A, Clotet B, Cooper D, Reynes J, Arasteh K, Nelson M, et al. Efficacy of enfuvirtide in patients infected with drug-resistant HIV-1 in Europe and Australia. New England Journal of Medicine 2003;348:2186–95.
Lohrengel S, Hermann F, Hagmann I, Oberwinkler H, Scrivano L, Hoffmann C, et al. Determinants of human immunodeficiency virus type 1 resistance to membrane-anchored gp41-derived peptides. Journal of Virology 2005;79:10237–46.
Loutfy MR, Raboud JM, Montaner JS, Antoniou T, Wynhoven B, Smaill F, et al. Assay of HIV gp41 amino acid sequence to identify baseline variation and mutation development in patients with virologic failure on enfuvirtide. Antiviral Research 2007;75:58–63.
Malashkevich VN, Chan DC, Chutkowski CT, Kim PS. Crystal structure of the simian immunodeficiency virus (SIV) gp41 core: conserved helical interactions underlie the broad inhibitory activity of gp41 peptides. Proceedings of the National Academy of Sciences of the United States of America 1998;95:9134–9.
Melby T, Sista P, DeMasi R, Kirkland T, Roberts N, Salgo M, et al. Characterization of envelope glycoprotein gp41 genotype and phenotypic susceptibility to enfuvirtide at baseline and on treatment in the phase III clinical trials TORO-1 and TORO-2. AIDS Research and Human Retroviruses 2006;22:375–85.
Mink M, Mosier SM, Janumpalli S, Davison D, Jin L, Melby T, et al. Impact of human immunodeficiency virus type 1 gp41 amino acid substitutions selected during enfuvirtide treatment on gp41 binding and antiviral potency of enfuvirtide in vitro. Journal of Virology 2005;79:12447–54.
Nameki D, Kodama E, Ikeuchi M, Mabuchi N, Otaka A, Tamamura H, et al. Mutations conferring resistance to human immunodeficiency virus type 1 fusion inhibitors are restricted by gp41 and Rev-responsive element functions. Journal of Virology 2005;79:764–70.
Nishikawa H, Nakamura S, Kodama E, Ito S, Kajiwara K, Izumi K, et al. Electrostatically constrained alpha-helical peptide inhibits replication of HIV-1 resistant to enfuvirtide. International Journal of Biochemistry and Cell Biology 2009;41:891–9.
Oishi S, Ito S, Nishikawa H, Watanabe K, Tanaka M, Ohno H, et al. Design of a novel HIV-1 fusion inhibitor that displays a minimal interface for binding affinity. Journal of Medicinal Chemistry 2008;51:388–91.
Oliveira AC, Martins AN, Pires AF, Arruda MB, Tanuri A, Pereira HS, et al. Enfuvirtide (T-20) resistance-related mutations in HIV type 1 subtypes B, C, and F isolates from Brazilian patients failing HAART. AIDS Research and Human Retroviruses 2009;25:193–8.
Otaka A, Nakamura M, Nameki D, Kodama E, Uchiyama S, Nakamura S, et al. Remodeling of gp41-C34 peptide leads to highly effective inhibitors of the fusion of HIV-1 with target cells. Angewandte Chemie International Edition in English 2002;41:2937–40.
Reeves JD, Gallo SA, Ahmad N, Miamidian JL, Harvey PE, Sharron M, et al. Sensitivity of HIV-1 to entry inhibitors correlates with envelope/coreceptor affinity, receptor density, and fusion kinetics. Proceedings of the National Academy of Sciences of the United States of America 2002;99:16249–54.
Shimura K, Nameki D, Kajiwara K, Watanabe K, Sakagami Y, Oishi S, et al. Resistance profiles of novel electrostatically constrained HIV-1 fusion inhibitors. Journal of Biological Chemistry 2010;285:39471–80.
Shirasaka T, Kavlick MF, Ueno T, Gao WY, Kojima E, Alcaide ML, Chokekijchai S, Roy BM, Arnold E, Yarchoan R, et al. Emergence of human immunodeficiency virus type 1 variants with resistance to multiple dideoxynucleosides in patients receiving therapy with dideoxynucleosides. Proceedings of the National Academy of Sciences of the United States of America 1995;92:2398–402.
Svicher V, Aquaro S, D'Arrigo R, Artese A, Dimonte S, Alcaro S, et al. Specific enfuvirtide-associated mutational pathways in HIV-1 Gp41 are significantly correlated with an increase in CD4(+) cell count, despite virological failure. Journal of Infectious Diseases 2008;197:1408–18.
Tolstrup M, Selzer-Plon J, Laursen AL, Bertelsen L, Gerstoft J, Duch M, et al. Full fusion competence rescue of the enfuvirtide resistant HIV-1 gp41 genotype (43D) by a prevalent polymorphism (137 K). AIDS 2007;21:519–21.
Ueno M, Kodama EN, Shimura K, Sakurai Y, Kajiwara K, Sakagami Y, et al. Synonymous mutations in stem-loop III of Rev responsive elements enhance HIV-1 replication impaired by primary mutations for resistance to enfuvirtide. Antiviral Research 2009;82:67–72.
Watabe T, Terakawa Y, Watanabe K, Ohno H, Nakano H, Nakatsu T, et al. X-ray crystallographic study of an HIV-1 fusion inhibitor with the gp41 S138A substitution. Journal of Molecular Biology 2009;392:657–65.
Welch BD, VanDemark AP, Heroux A, Hill CP, Kay MS. Potent D-peptide inhibitors of HIV-1 entry. Proceedings of the National Academy of Sciences of the United States of America 2007;104:16828–33.
Xu L, Pozniak A, Wildfire A, Stanfield-Oakley SA, Mosier SM, Ratcliffe D, et al. Emergence and evolution of enfuvirtide resistance following long-term therapy involves heptad repeat 2 mutations within gp41. Antimicrobial Agents and Chemotherapy 2005;49:1113–9.

Journal of Clinical Virology 58 (2013) 635–640

Contents lists available at ScienceDirect

Journal of Clinical Virology

journal homepage: www.elsevier.com/locate/jcv

Galectin-9 plasma levels reflect adverse hematological and immunological features in acute dengue virus infection☆

Haorile Chagan-Yasutan[a,b], Lishomwa C. Ndhlovu[c], Talitha Lea Lacuesta[d], Toru Kubo[e], Prisca Susan A. Leano[f], Toshiro Niki[g], Shigeru Oguma[h], Kouichi Morita[e], Glen. M. Chew[c], Jason D. Barbour[c], Elizabeth Freda O. Telan[f], Mitsuomi Hirashima[g], Toshio Hattori[a,b,*], Efren M. Dimaano[d]

[a] Laboratory of Disaster-Related Infectious Disease, International Research Institute of Disaster Science, Tohoku University, Sendai, Japan
[b] Division of Emerging Infectious Diseases, Department of Internal Medicine, Graduate School of Medicine, Tohoku University, Sendai, Japan
[c] Department of Tropical Medicine, John A. Burns School of Medicine, University of Hawaii, Manoa, USA
[d] Department of Blood Borne Diseases, San Lazaro Hospital, Manila, Philippines
[e] Department of Virology, Institute of Tropical Medicine, Nagasaki University, Nagasaki, Japan
[f] National Reference Laboratory for HIV/AIDS, Hepatitis, and other STDs, STD/AIDS Cooperative Central Laboratory, Manila, Philippines
[g] Department of Immunology and Immunopathology, Kagawa University, Takamatsu, Japan
[h] Medical Informatics Division, Takeda General Hospital, Kyoto, Japan

ARTICLE INFO

Article history:
Received 15 May 2013
Received in revised form
29 September 2013
Accepted 18 October 2013

Keywords:
Galectin-9
Dengue virus
Biomarker
Dengue fever
Dengue hemorrhagic fever

ABSTRACT

Background: Dengue virus (DENV) infection remains a major public health burden worldwide. Soluble mediators may play a critical role in the pathogenesis of acute DENV infection. Galectin-9 (Gal-9) is a soluble β-galactoside-binding lectin, with multiple immunoregulatory and inflammatory properties.
Objective: To investigate plasma Gal-9 levels as a biomarker for DENV infection.
Study design: We enrolled 65 DENV infected patients during the 2010 epidemic in the Philippines and measured their plasma Gal-9 and cytokine/chemokine levels, DENV genotypes, and copy number during the critical and recovery phases of illness.
Results: During the critical phase, Gal-9 levels were significantly higher in DENV infected patients compared to healthy or those with non-dengue febrile illness. The highest Gal-9 levels were observed in dengue hemorrhagic fever (DHF) patients (DHF: 2464 pg/ml; dengue fever patients (DF): 1407 pg/ml; non-dengue febrile illness: 616 pg/ml; healthy: 196 pg/ml). In the recovery phase, Gal-9 levels significantly declined from peak levels in DF and DHF patients. Gal-9 levels tracked viral load, and were associated with multiple cytokines and chemokines (IL-1α, IL-8, IP-10, and VEGF), including monocyte frequencies and hematologic variables of coagulation. Further discriminant analyses showed that eotaxin, Gal-9, IFN-α2, and MCP-1 could detect 92% of DHF and 79.3% of DF, specifically ($P < 0.01$).
Conclusion: Gal-9 appears to track DENV inflammatory responses, and therefore, it could serve as an important novel biomarker of acute DENV infection and disease severity.

1. Background

Dengue is caused by the dengue virus (DENV), which belongs to the family Flaviviridae, genus *Flavivirus*, and is now emerging as one of the most rapidly spreading mosquito-borne viral diseases worldwide.[1,2] DENV has an incubation period of 3–7 days, where after the symptoms suddenly appear. Clinically, the onset of symptoms is rapid and follows 3 distinct phases: (1) an initial febrile phase on days 1–3 of illness; (2) a critical phase on days 4–6 of illness, which coincides with defervescence; and (3) a spontaneous recovery phase on days 7–10 of illness. Dengue fever (DF) is accompanied by a high fever, headaches, severe myalgia, and rash. Severe DENV infection complications can occur resulting in dengue hemorrhagic fever (DHF), which is characterized with clinical and laboratory features of thrombocytopenia, coagulation abnormalities, and plasma leakage in children and worse outcomes in adults

* Corresponding author at: Laboratory of Disaster-Related Infectious Disease, International Research Institute of Disaster Science, Tohoku University, 2-1 Seiryo-cho, Aoba-ku, Sendai 980-8575, Japan. Tel.: +81 22 717 8220; fax: +81 22 717 8221.
E-mail address: hatoriaoi@gmail.com (T. Hattori).

1386-6532/$ – see front matter © 2013 The Authors. Published by Elsevier B.V. All rights reserved.
http://dx.doi.org/10.1016/j.jcv.2013.10.022

presenting with increased incidences of bleeding, shock and organ failure.[3,4]

It is thought that following acute DENV infection, the high viral load triggers an activated immunological state, resulting in the release of inflammatory cytokines, chemokines, immune complexes, and other inflammatory mediators.[5] During the evolution of DENV infection, both pro-inflammatory and anti-inflammatory cytokines and chemokines are induced, suggesting that multifactorial mediators are also involved in DENV-induced pathogenesis.[6–8]

Galectins constitute a family of mammalian lectins that have an affinity for β-galactoside. These proteins are released into the extra-cellular environment under stress conditions such as infectious, during which they serve as "danger signals" or exert their actions on other cells.[9] Galectin-9 (Gal-9) was first described as an eosinophilic chemoattractant.[10,11] Since then, Gal-9 is reported to be produced by both T and endothelial cells,[12,13] and its functions as a bidirectional immunoregulator was recently described.[14,15] We previously described increases in Gal-9 and histamine levels in an allergic patient and suggested that the activation of mast cells is associated with elevation in Gal-9 levels.[16] We also reported a marked elevation of Gal-9 in acute human immunodeficiency virus (HIV) infection and a rapid decrease after anti-retroviral therapy, and our data from that study suggested that Gal-9 could be a potential danger signal biomarker of acute virus infection.[17,18]

2. Objectives

To examine the kinetics and activities of Gal-9 in DENV infection and its association with other circulating plasma mediators during the course of acute DENV infection.

3. Study design

3.1. Patients and specimens

We conducted a study at the San Lazaro Hospital in Manila, Philippines, which included 65 serially recruited patients with a clinical diagnosis of DF and DHF.[19] In 2010, there were consecutive cases of dengue in this hospital, and we enrolled patients who met the study's inclusion criteria. None of the patients included in our study died, and all of them were discharged from the hospital when their condition improved. EDTA plasma and serum were obtained by centrifugation of peripheral blood at 3000 rpm for 10 min, and were aliquoted into 1.2 ml micro tubes and stored at −80 °C until use. Specimens were collected at 2 time points during illness of the critical phase (on days 4–5) and the recovery phase (on days 7–8). All enrolled patients underwent laboratory tests, their medical histories were recorded, and they were physically examined by resident clinicians. Plasma was also obtained from 30 demographically matched healthy controls (HCs). HCs were donors who came to the Hospital for annual health checks or who volunteered at the Hospital. In addition, 90 patients with non-dengue febrile illness, who had visited San Lazaro Hospital, were enrolled. These patients were clinically diagnosed with leptospirosis, confirmed by serological analysis and/or microscopic agglutination test.[20] Plasma from patients with non-dengue febrile illness was collected at the time of admission.

3.2. Serological analysis

Primary and secondary DENV infections were confirmed by determining antiviral IgM and/or IgG antibodies levels using sera (The Panbio Duo Dengue IgM and IgG Capture enzyme-linked immunosorbent assay (ELISA), Panbio, Queensland, Australia).[21]

3.3. RNA extraction

Genomic viral RNA was extracted from 140 μl of each patient serum (critical phase, $n=65$) using the QIAamp viral RNA mini kit (QIAGEN, Hilden, Germany). The extracted RNA was stored at −80 °C until further use.

3.4. DENV genotyping

DENV genotyping was performed by the dengue genotype-specific reverse transcriptase loop-mediated isothermal amplification (RT-LAMP) method.[22] The RT-LAMP reaction was carried out in a 25 μl reaction mixture with the use of the Loopamp RNA Amplification Kit (Eiken Chemical Co., Ltd., Tokyo, Japan), and it was performed with 1 μl of template RNA. The reaction mix was incubated at 60 °C for 60 min in a Loopamp real-time turbidometer LA-320C (Teramecs, Kyoto, Japan). Positive and negative controls were included in each run, and all precautions to prevent cross-contamination were taken. The results were confirmed by LA-320C software.

3.5. Real-time RT-PCR and DENV quantification

The DENV copy number in plasma was measured by a TaqMan® one-step real-time RT-PCR as described previously.[23] The real-time RT-PCR primers and hydrolysis probe specific to the 3′ untranslated region (UTR) of the four-dengue genotypes were described previously.[24] In this study, hydrolysis probe was labeled by FAM at the 5′ end and BHQ-1 at the 3′ end. The real-time RT-PCR assay was performed using the SuperScript® III Platinum One-Step qRT-PCR Kit (Invitrogen, USA), according to the manufacturer's instructions. Quantitative standard RNA or each DENV genotype was performed using the *in vitro* transcription of the pCR®2.1-TOPO® vector (Invitrogen, USA), which was cloned at the 3′ UTR for each DENV genotype: genotype 1 (strain 99St-12A; GenBank accession no GU377286), genotype 2 (00St-22A; GU377287), genotype 3 (SLMC50; GU377288), and genotype 4 (SLMC318; GU377289), respectively. The target RNA copy number was calculated, and 10-fold serial dilutions ranging from 10^2 to 10^5 RNA copies per microliter were used for quantification standards. One microliter of RNA standard or extracted RNA was used as template per reaction. Virus titer in each reaction was calculated using 7500 System Software (Applied Biosystems, USA).

3.6. Galectin-9 and cytokine/chemokines detection assay

Plasma Gal-9 was quantified by means of ELISA, as previously described.[17] Briefly, the sandwich ELISA consists of anti-human Gal-9 monoclonal antibodies (clone 9S2-3; GalPharma, Takamatsu, Japan) and biotinylated-anti-human Gal-9 polyclonal antibodies (GalPharma, Takamatsu, Japan) as a coating and detection antibodies, respectively. Colorimetric analysis was carried out using streptavidin-conjugated horseradish peroxidase (Thermo Fisher Scientific, Waltham, MA, USA) and tetramethyl benzidine (KPL, Gaithersburg, MD, USA). Gal-9 concentration was quantified using a standard curve constructed with recombinant human Gal-9 (GalPharma, Takamatsu, Japan). Plasma samples were also assayed for 29 selected cytokines and chemokines (EGF, eotaxin, G-CSF, GM-CSF, IFN-α2, IFN-γ, IL-10, IL-12p40, IL-12p70, IL-13, IL-15, IL-17, IL-1ra, IL-1α, IL-1β, IL-2, IL-3, IL-4, IL-5, IL-6, IL-7, IL-8, IP-10, MCP-1, MIP-1α, MIP-1β, TNF-α, TNF-β, and VEGF) using a Milliplex Human Cytokine and Chemokine multiplex assay Kit (Merck Millipore, Billerica, MA, USA). The experiments were performed according to the manufacturers' instructions using a Luminex 200 System (Luminex Corporation, Austin, USA).[25]

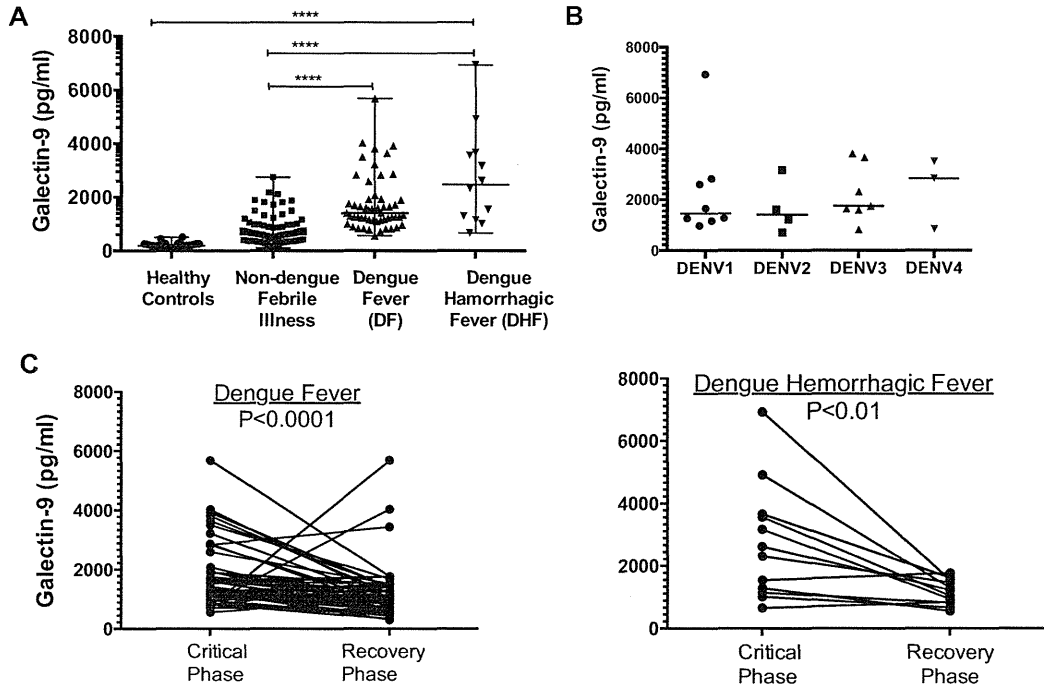

Fig. 1. Plasma levels of galectin-9 in dengue virus infected individuals. (A) Significantly different levels of plasma galectin-9 in the critical phase of patients with DF and DHF as well as in non-dengue febrile illness (patients with leptospirosis) and healthy controls (Kruskal–Wallis test, $P < 0.0001$). Dunn's multiple comparison tests showed significant differences between healthy controls and DF/DHF patients ($P < 0.001$), and between non-dengue febrile illness and DF/DHF. (B) No significant differences in galectin-9 levels between 4 serotypes (Kruskal–Wallis test). (C) Changes in the plasma levels of galectin-9 from the critical to recovery phases in patients with DF and DHF. Abbreviations: DF, dengue fever; DHF, dengue hemorrhagic fever.

3.7. Statistical analysis

We tested for differences in plasma Gal-9 levels between groups (DF, DHF, non-dengue febrile illness, and HCs) using the Kruskal–Wallis test and between the critical and recovery phases of DENV infection with the Wilcoxon signed-ranks test. Differences in the clinical data between patients with DF and DHF and cytokine/chemokine levels between patients and HCs were assessed by the Mann–Whitney test. These statistical analyses were performed using GraphPad Prism 6 software (GraphPad Software, San Diego, CA, USA). In addition, a stepwise discriminant analysis was used to differentiate DHF from DF patients using Gal-9 and other cytokine/chemokines. Furthermore, to determine the variables that independently associated with Gal-9 in the DENV infected patients, a stepwise multiple regression analysis was performed. Multivariable analyses were conducted using the Ekuseru-Toukei 2012 software (Social Survey Research Information Co., Ltd., Tokyo, Japan).

4. Results

4.1. Basic and clinical characteristics of the acute DENV infected patients

The mean age of the patients with DENV infection ($n = 65$), non-dengue febrile illness ($n = 90$), and HCs ($n = 30$) were 23.5, 33.4, and 33.7 years, respectively. All DENV infected patients had anti-DENV IgG and/or IgM. Secondary infection that was caused by preexisting IgG antibodies was confirmed in 62% of the total group of patients. Secondary infection was seen in 57% and 83% of patients with DF and DHF, respectively. Patients with DHF had significantly lower platelet counts and significantly higher Hct levels than patients with DF.

4.2. Assessment of DENV genotype and viral RNA copy number

We identified dengue genotypes in 27 of the 65 samples (42%) by LAMP methods. Amongst the 27 patients, DENV 1, 2, 3, and 4 were found in 13, 4, 7, and 3 of the patients, respectively. Of the 27, 16 (59%) and 10 (37%) were found to have primary and secondary infections, respectively.

4.3. Increased levels of plasma Gal-9 in the DENV infection

In the critical phase, plasma Gal-9 levels were a significantly elevated in the DENV infected patients compared to those with non-dengue febrile illness and HCs ($P < 0.0001$, Kruskal–Wallis test, Fig. 1A). The median plasma Gal-9 levels for DENV infected, non-dengue febrile patients, and HCs were 1525, 616, and 196 pg/ml, respectively. The increase in Gal-9 in DENV infected patients was found to be apparently associated with disease severity (1407 pg/ml in DF and 2464 pg/ml in DHF patients). Gal-9 levels in the 4 genotypes were also elevated to a similar extent (Fig. 1B), and to our knowledge, these levels appear to be amongst the highest ever reported in humans.

During the recovery phase, Gal-9 levels significantly declined overall to a median of 1010 pg/ml in all patients, except in 6 with DF. The median level of Gal-9 in patients with DF and DHF during the recovery phase was 1002 pg/ml and 1126 pg/ml, respectively (Fig. 1C).

4.4. Numerous cytokines and chemokines were elevated in DENV infection and were associated with Gal-9 levels

We measured 29 cytokines and chemokines using a multiplex bead assay in all 65 patients (both in the critical as well as the recovery phase of infection) in comparison to 30 HCs. In

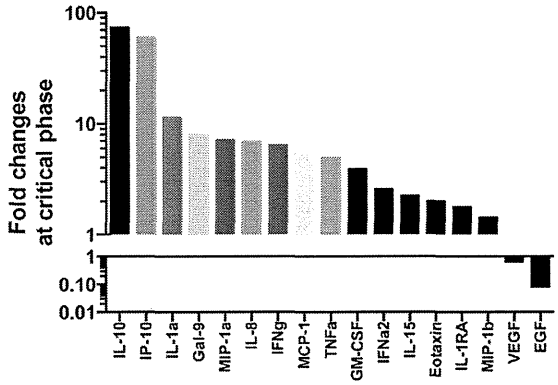

Fig. 2. Significant changes in cytokine/chemokine and galectin-9 levels in DENV infected patients. Median fold changes in galectin-9 and cytokine/chemokine levels were calculated as: median of the critical phase from DENV infected patients/median of HCs. The differences between the levels of patients and HCs were evaluated by Mann–Whitney test. DENV, dengue virus; HCs, healthy controls.

the critical phases of DENV infection, we found that 16 cytokines and chemokines, significantly changed compared to HCs, with the levels of IL-10, IP-10, and IL-1α having the greatest increase in relation to Gal-9 levels (Fig. 2). The levels of 2 growth factors, VEGF, and EGF declined. However, the median levels of other 13 cytokines and chemokines remained unchanged compared to HCs. All cytokines and chemokines that were elevated in the critical phase decreased in the recovery phase with the exception of eotaxin, which remained persistently high. The levels of VEGF and EGF remained low even into the recovery phase of infection.

A stepwise discriminant analysis was used to differentiate DHF from DF patients, in order to ascertain whether Gal-9 is an independent variable in DENV infection. Specifically, DF/DHF was set as a dependent variable, and Gal-9 and other cytokine/chemokines were set as independent variables. The result showed that eotaxin, Gal-9, IFN-α2, and MCP-1 could detect 92% of DHF and 79.3% of DF, specifically ($P<0.01$). Furthermore, using multiple regression analysis, we found that during the critical phase of infection, Gal-9 was significantly associated with IL-1α ($P<0.05$), IL-8 ($P<0.001$), IP-10 ($P<0.01$), and VEGF ($P<0.05$) (Fig. 3A), and during the recovery phase Gal-9 was significantly associated with EGF ($P<0.01$), IL-10 ($P<0.05$), IL-8 ($P<0.05$), and VEGF ($P<0.05$) (Fig. 3B).

4.5. Association of plasma Gal-9 levels with clinical variables of DENV infection

We next assessed whether plasma Gal-9 levels were associated with the hematological variables of DENV infection using multiple regression analysis. In both the critical and recovery phases of DENV infection, we observed that Gal-9 levels were positively associated with Hematocrit (Hct), and inversely associated with platelet counts. Furthermore, monocyte and viral RNA copy numbers were also associated with plasma Gal-9 levels (Fig. 3C and D).

5. Discussion

Our results reveal for the first time the dynamic of Gal-9 release in acute DENV infection. During the critical phase of acute DENV infection, plasma Gal-9 levels were markedly elevated compared to those in non-dengue febrile illness and HCs. The levels significantly declined during the recovery phase, indicating resolution of inflammation. We identified all 4 DENV genotypes in this cohort in line with that previously reported in the Philippines[26] and demonstrated no preferential regulation of Gal-9 by

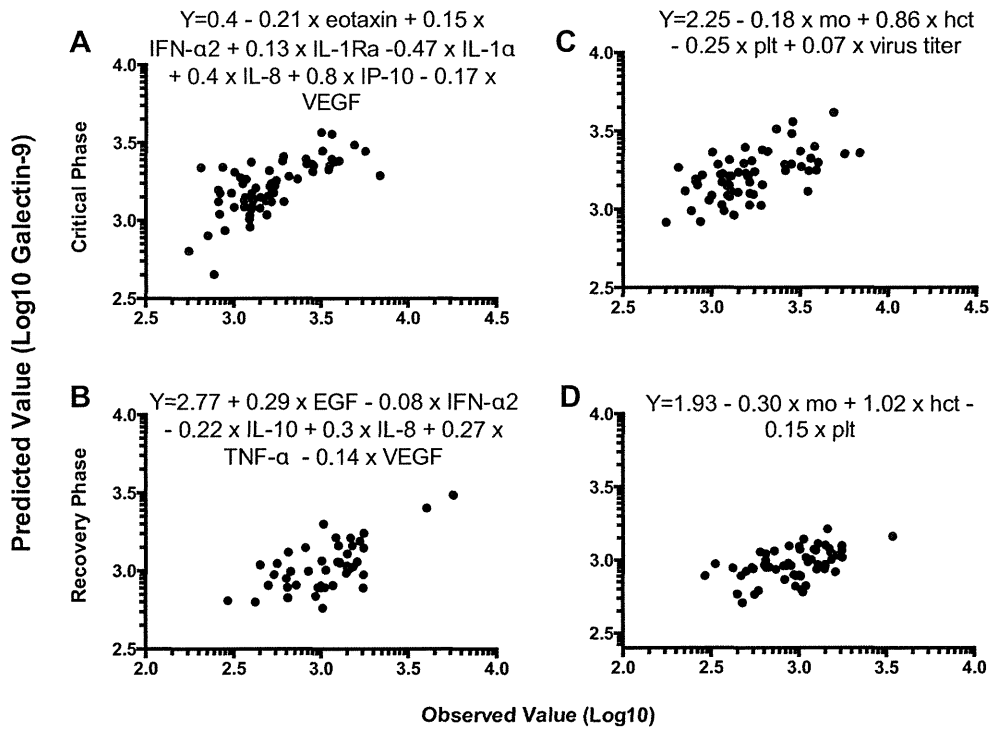

Fig. 3. Results of stepwise multiple regression analysis when galectin-9 was set as a dependent variable. Significantly elevated cytokine/chemokines such as IL-10, IP-10, IL-1α, MIP-1α, IL-8, IFN-g, MCP-1, TNF-α, GM-CSF, IFN-α2, IL-15, eotaxin, IL-1Ra, MIP-1b, VEGF, and EGF were included as independent variables in models A and B. WBC, lymphocyte, monocyte, neutrophil, RBC, Hg, Hct, and Plt were used as independent variables in models C and D; virus titers were only obtained in the critical phase (C). Abbreviations: mo, monocyte; Hct, hematocrit; Plt, platelet count.

genotype. Multiplex analysis showed 16 out of 29 cytokines and chemokines were significant different compared to HCs during the critical phase. Gal-9 and above cytokines and chemokines might be released by activated macrophages and endothelial cells following DENV infection. The Gal-9 levels were inversely correlated with monocyte percentages in patients with DENV infection. Therefore, we assumed that monocytes migrate and attach to inflamed endothelial cells. Released Gal-9 may further activate monocytes in autocrine manner.[27]

Gal-9 levels were also associated with platelet counts and hematocrit levels in both critical and recovery phases. As a family, galectins serve as "danger signals" that exert their actions on several immune cell populations, including mast cells.[28] The association of Gal-9 with dengue virus titers in the present study results supports this hypothesis. Further, the activation of mast cells is important because these cells secrete histamine, which enhance the permeability of endothelial cells. We previously reported a possible association between Gal-9 and histamine release in an allergic patient.[16] However, other mast cell-derived mediators such as VEGF, tryptase, and chymase have been reported to participate in the development of DHF.[29] In fact, Gal-9 levels were associated with VEGF and also with other macrophage derived inflammatory molecules such as IL-8 and IP-10.

From our data, it is evident that DENV viral content could regulate the profound increase in circulating Gal-9 levels and the diverse cytokine and chemokine storm associated with Gal-9. Acute HIV, unlike acute HCV or HBV, leads to a rapid cytokine storm.[30] We have shown that Gal-9 levels are greatly elevated in acute HIV infection[17] and recently found it appears to be related to HIV virus titers (data not shown) suggesting similar mechanisms may be occurring. In the present study, we found that non-virus pathogenic agents can upregulate Gal-9: patients with leptospirosis had elevated Gal-9 levels compared to those with HCs, although this elevation was not as high as that in patients with DENV or acute HIV. Further studies investigating Gal-9 in various infectious diseases is necessary to clarify the biological nature underlying the elevation of Gal-9 in DENV infection.

The limitation of our study was the small number of patients with DENV and non-age matched HCs included in our study. The precise role of Gal-9 in DENV infection requires a large-scale longitudinal study that includes patients with serious symptoms such as dengue shock syndrome. Taken together, the present study shows that plasma levels of Gal-9 appears to track DENV inflammatory responses and could serve as an important novel biomarker of acute DENV infection and disease severity.

Funding

This study was supported by the Ministry of Education, Science and Culture (Grants-in-Aid for Scientific Research: Fundamental Research A, grant number 23256004, Overseas Academic Investigation), a JSPS Overseas Scientific Grant for Young Investigators (H.C.-Y.) and a special research grant from IRIDeS. The project was supported in part by the National Institute on Minority Health and Health Disparities (U54MD007584), National Institutes of Health (NIH).

Competing interest

All authors declare that they have no conflicts of interest.

Ethical approval

The study was conducted in accordance with the Declaration of Helsinki and was approved by the Ethics Committee of San Lazaro Hospital, Manila, Philippines (2009-003) (2011-08-010) and the Tohoku University Hospital, Sendai, Japan (2009-425) (2013-1-224) and Human Studies Program of the University of Hawaii, USA (CHS 20982). Written informed consent was obtained from all study participants.

Acknowledgements

We thank the patients and the volunteers who participated in this study. The authors also thank Bonnie Brayton from the University of Hawaii for her invaluable technical assistance in the multiplex bead assay.

References

1 Bhatt S, Gething PW, Brady OJ, Messina JP, Farlow AW, Moyes CL, et al. The global distribution and burden of dengue. Nature 2013;496:504–7.
2 Nathan MB, Dayal-Drager R, Guzman M. Epidemiology, burden of disease and transmission. Dengue, guidelines for diagnosis, treatment, prevention and control new edition. Geneva: World Health Organization; 2009. p. 3–21.
3 Simmons CP, Farrar JJ, Nguyen vV, Wills B. Dengue. N Engl J Med 2012;366:1423–32.
4 Trung DT, Thao le TT, Dung NM, Ngoc TV, Hien TT, Chau NV, et al. Clinical features of dengue in a large Vietnamese cohort: intrinsically lower platelet counts and greater risk for bleeding in adults than children. PLoS Negl Trop Dis 2012;6:e1679.
5 Martina BE, Koraka P, Osterhaus AD. Dengue virus pathogenesis: an integrated view. Clin Microbiol Rev 2009;22:564–81.
6 Appanna R, Wang SM, Ponnampalavanar SA, Lum LC, Sekaran SD. Cytokine factors present in dengue patient sera induces alterations of junctional proteins in human endothelial cells. Am J Trop Med Hyg 2012;87:936–42.
7 Becquart P, Wauquier N, Nkoghe D, Ndjoyi-Mbiguino A, Padilla C, Souris M, et al. Acute dengue virus 2 infection in Gabonese patients is associated with an early innate immune response, including strong interferon alpha production. BMC Infect Dis 2010;10:356.
8 Guerrero CD, Arrieta AF, Ramirez ND, Rodriguez LS, Vega R, Bosch I, et al. High plasma levels of soluble ST2 but not its ligand IL-33 is associated with severe forms of pediatric dengue. Cytokine 2013;61:766–71.
9 Vasta GR, Ahmed H, Nita-Lazar M, Banerjee A, Pasek M, Shridhar S, et al. Galectins as self/non-self recognition receptors in innate and adaptive immunity: an unresolved paradox. Front Immunol 2012;3:199.
10 Matsumoto R, Matsumoto H, Seki M, Hata M, Asano Y, Kanegasaki S, et al. Human ecalectin, a variant of human galectin-9, is a novel eosinophil chemoattractant produced by T lymphocytes. J Biol Chem 1998;273:16976–84.
11 Tureci O, Schmitt H, Fadle N, Pfreundschuh M, Sahin U. Molecular definition of a novel human galectin which is immunogenic in patients with Hodgkin's disease. J Biol Chem 1997;272:6416–22.
12 Chabot S, Kashio Y, Seki M, Shirato Y, Nakamura K, Nishi N, et al. Regulation of galectin-9 expression and release in Jurkat T cell line cells. Glycobiology 2002;12:111–8.
13 Warke RV, Xhaja K, Martin KJ, Fournier MF, Shaw SK, Brizuela N, et al. Dengue virus induces novel changes in gene expression of human umbilical vein endothelial cells. J Virol 2003;77:11822–32.
14 Anderson AC, Anderson DE, Bregoli L, Hastings WD, Kassam N, Lei C, et al. Promotion of tissue inflammation by the immune receptor Tim-3 expressed on innate immune cells. Science 2007;318:1141–3.
15 Mengshol JA, Golden-Mason L, Arikawa T, Smith M, Niki T, McWilliams R, et al. A crucial role for Kupffer cell-derived galectin-9 in regulation of T cell immunity in hepatitis C infection. PLoS ONE 2010;5:e9504.
16 Chagan-Yasutan H, Shiratori B, Siddiqi UR, Saitoh H, Ashino Y, Arikawa T, et al. The increase of plasma galectin-9 in a patient with insulin allergy: a case report. Clin Mol Allergy 2010;8:12.
17 Chagan-Yasutan H, Saitoh H, Ashino Y, Arikawa T, Hirashima M, Li S, et al. Persistent elevation of plasma osteopontin levels in HIV patients despite highly active antiretroviral therapy. Tohoku J Exp Med 2009;218:285–92.
18 Saitoh HAY, Chagan-Yasutan H, Niki T, Hirashima M, Hattori T. Rapid decrease of plasma galectin-9 levels in patient with acute HIV infection after therapy. Tohoku J Exp Med 2012;228:157–61.
19 WHO. Dengue haemorrhagic fever-diagnosis, treatment, prevention and control. World Health Organization; 1997.
20 Masuzawa T, Dancel LA, Miyake M, Yanagihara Y. Serological analysis of human leptospirosis in the Philippines. Microbiol Immunol 2001;45:93–5.
21 Vaughn DW, Nisalak A, Solomon T, Kalayanarooj S, Dung NM, Kneen R, et al. Rapid serologic diagnosis of dengue virus infection using a commercial capture ELISA that distinguishes primary and secondary infections. Am J Trop Med Hyg 1999;60:693–8.
22 Parida M, Horioke K, Ishida H, Dash PK, Saxena P, Jana AM, et al. Rapid detection and differentiation of dengue virus serotypes by a real-time reverse transcription-loop-mediated isothermal amplification assay. J Clin Microbiol 2005;43:2895–903.

23 Kubo T, Agoh M, Mai le Q, Fukushima K, Nishimura H, Yamaguchi A, et al. Development of a reverse transcription-loop-mediated isothermal amplification assay for detection of pandemic (H1N1) 2009 virus as a novel molecular method for diagnosis of pandemic influenza in resource-limited settings. J Clin Microbiol 2010;48:728–35.
24 Warrilow D, Northill JA, Pyke A, Smith GA. Single rapid TaqMan fluorogenic probe based PCR assay that detects all four dengue serotypes. J Med Virol 2002;66:524–8.
25 Garg AD, Krysko DV, Verfaillie T, Kaczmarek A, Ferreira GB, Marysael T, et al. A novel pathway combining calreticulin exposure and ATP secretion in immunogenic cancer cell death. EMBO J 2012;31:1062–79.
26 Manaloto CR, Hayes CG. Isolation of dengue viruses from hospitalized patients in the Philippines, 1983–1986. Southeast Asian J Trop Med Public Health 1989;20:541–7.
27 Matsuura A, Tsukada J, Mizobe T, Higashi T, Mouri F, Tanikawa R, et al. Intracellular galectin-9 activates inflammatory cytokines in monocytes. Genes Cells 2009;14:511–21.
28 Sato S, Nieminen J. Seeing strangers or announcing "danger": galectin-3 in two models of innate immunity. Glycoconj J 2004;19:583–91.
29 Furuta T, Murao LA, Lan NT, Huy NT, Huong VT, Thuy TT, et al. Association of mast cell-derived VEGF and proteases in Dengue shock syndrome. PLoS Negl Trop Dis 2012;6:1505e.
30 Stacey AR, Norris PJ, Qin L, Haygreen EA, Taylor E, Heitman J, et al. Induction of a striking systemic cytokine cascade prior to peak viremia in acute human immunodeficiency virus type 1 infection, in contrast to more modest and delayed responses in acute hepatitis B and C virus infections. J Virol 2009;83:3719–33.

Kadowaki et al. Critical Care 2013, 17:R284
http://ccforum.com/content/17/6/R284

CRITICAL CARE

RESEARCH Open Access

Galectin-9 prolongs the survival of septic mice by expanding tim-3-expressing natural killer T cells and PDCA-1$^+$ CD11c$^+$ macrophages

Takashi Kadowaki[1†], Asahiro Morishita[2†], Toshiro Niki[1], Junko Hara[3], Miwa Sato[3], Joji Tani[2], Hisaaki Miyoshi[2], Hirohito Yoneyama[2], Tsutomu Masaki[2], Toshio Hattori[4], Akihiro Matsukawa[3] and Mitsuomi Hirashima[2,5*]

Abstract

Introduction: Galectin-9 ameliorates various inflammatory conditions including autoimmune diseases by regulating T cell and macrophage/dendritic cell (DC) functions. However, the effect of galectin-9 on polymicrobial sepsis has not been assessed.

Methods: We induced polymicrobial sepsis by cecal ligation and puncture (CLP) in mice. The survival rate was compared between galectin-9- and PBS-treated CLP mice. An ELISA was used to compare the levels of various cytokines in the plasma and culture supernatants. Fluorescence-activated cell sorting analysis was further performed to compare the frequencies of subpopulations of spleen cells.

Results: Galectin-9 exhibited a protective effect in polymicrobial sepsis as demonstrated in galetin-9 transgenic mice and therapeutic galectin-9 administration. In contrast, such effect was not observed in nude mice, indicating the involvement of T cells in galectin-9-mediated survival prolongation. Galectin-9 decreased TNFα, IL-6, IL-10 and, high mobility group box 1 (HMGB1) and increased IL-15 and IL-17 plasma and spleen levels. Galectin-9 increased the frequencies of natural killer T (NKT) cells and PDCA-1$^+$ CD11c$^+$ macrophages (pDC-like macrophages) but did not change the frequency of CD4 or CD8 T cells, γδT cells or conventional DC. As expected, galectin-9 decreased the frequency of Tim-3$^+$ CD4 T cells, most likely Th1 and Th17 cells. Intriguingly, many spleen NK1.1$^+$ NKT cells and pDC-like macrophages expressed Tim-3. Galectin-9 increased the frequency of Tim-3-expressing NK1.1$^+$ NKT cells and pDC-like macrophages. Galectin-9 further increased IL-17$^+$ NK1.1$^+$ NKT cells.

Conclusion: These data suggest that galectin-9 exerts therapeutic effects on polymicrobial sepsis, possibly by expanding NKT cells and pDC-like macrophages and by modulating the production of early and late proinflammatory cytokines.

Introduction

Sepsis is the leading cause of death in critically ill patients, and the incidence of sepsis is increasing. The mortality rate of severe sepsis is very high, up to 70%. Two types of animal sepsis model have been established: the lipopolysaccharide(LPS)-induced inflammation, and the cecal ligation and puncture (CLP) model of microbial sepsis. LPS stimulates macrophages to release large amounts of TNFα and IL-1β that can precipitate tissue injury and lethal shock. Antagonists of TNFα and IL-1β have shown limited efficacy in clinical trials, most likely because these cytokines are early mediators in sepsis pathogenesis [1,2].

On the other hand, high mobility group box 1 (HMGB1) is thought to be a late mediator of endotoxin lethality in mice, and HMGB1 is first detectable in the circulation 8 hours after the onset of sepsis disease, subsequently increasing to plateau levels from 16 to 32 hours [3]. Administration of HMGB1-specific neutralizing antibodies beginning 24 hours after the onset of sepsis induced by CLP was shown to lead to a dose-dependent rescue of mice from lethal sepsis [4-6].

* Correspondence: mitsuomi@kms.a
†Equal contributors
[2]Department of Gastroenterology and Neurology, Kagawa University Faculty of Medicine, Kagawa, Japan
[5]Laboratory of Biodefense Research, Faculty of Pharmaceutical Sciences at Kagawa Campus, Tokushima Bunri University, Kagawa, Japan
Full list of author information is available at the end of the article

Recent studies have also shown that programmed death-1 (PD-1) expression on macrophages is critically associated with altering microbial clearance and the innate inflammatory response to sepsis in CLP mice [7]. Upregulation of PD-1 on T cells and the PD-ligand (L) 1 on monocytes in patients with septic shock has also been observed [8], and it has been shown that PD-1 levels correlate with increased mortality, nosocomial infections, and immune dysfunction in patients with septic shock [9]. Moreover, blockade of the PD-1/PD-L1 pathway improves survival in CLP mice by reversing immune dysfunction [10-12].

Galectin-9 (Gal-9) is a member of the galectin family that selectively binds to β-galactoside [13]. Gal-9 was first identified as an apoptosis-inducing factor for thymocytes [14] and an eosinophil-activating factor [15]. However, recent experiments have revealed that Gal-9 is a ligand of Tim-3 that is expressed on Th1 and Th17 cells, and that Gal-9 signaling induces death of these cells, resulting in the suppression of Th1- and Th17-related cytokine production *in vivo* and *in vitro* [16,17]. More recently, it has been shown that Gal-9 derived from surface Gal-9-expressing Th cells (ThGal-9) suppresses the development of Th17 cells and enhances the development of $FoxP3^+$ regulatory T cells (Tregs) in a Tim-3-independent manner [18]. In addition to the above mechanisms, Gal-9 modulates immune responses by expanding myeloid suppressor cells [19] and plasmacytoid dendritic cell (pDC)-like macrophages [20-23]. We have also shown that Gal-9 ameliorates LPS-induced inflammation and protects mice from an LPS-induced Schwartzman reaction by suppressing the production of proinflammatory cytokines from LPS-stimulated macrophages and activating PGE2-producing neutrophils, respectively [24]. Therefore, it is of interest to examine the role of Gal-9 in a murine model of polymicrobial sepsis induced by CLP. The purpose of the present experiment is to show a beneficial effect of Gal-9 in a murine sepsis model induced by CLP and to clarify possible functions of Gal-9 in this model.

Materials and methods

Mice

Female wild-type (WT) Balb/c mice and Gal-9 transgenic (TG) mice were used in the present study [24]. These mice were maintained on a 12:12-hour light–dark cycle under specific pathogen-free conditions at Kagawa University. The animals were fed a standard laboratory diet and were provided water *ad libitum*. All experimental procedures were approved by the Animal Care and Use Committee of Kagawa University. The animals used in this research received humane care in accordance with international guidelines and national law.

Induction of sepsis

CLP appears to be a reliable and clinically relevant animal model of the human septic condition because it produces an endogenous polymicrobial infection similar to clinical peritonitis and sepsis. Thus, sepsis was induced by CLP in the present experiments as described elsewhere [25]. Briefly, mice were anesthetized, and the cecum was exposed, ligated with a 3–0 silk suture and punctured once with an 18-gauge needle. The cecum was then replaced in the peritoneal cavity, and the incision was closed with surgical staples. All mice received a subcutaneous injection of 1 ml of sterile saline to avoid dehydration and were placed on a heating pad until they recovered from anesthesia. All mice were allowed free access to food and water throughout the experiments. We used stable human Gal-9 [26] to assess the effects of Gal-9 on the survival of CLP mice. The purity of Gal-9 was >95%. The endotoxin level was determined using a Limulus assay (BioWhittaker, Tokyo, Japan) and was found to be <0.008 endotoxin units. CLP mice were treated with Gal-9 intravenously or subcutaneously immediately after CLP unless otherwise specified. To determine the survival of the mice, CLP mice were monitored for 7 days after CLP. In a different set of experiments, CLP mice were anesthetized, bled and euthanized at indicated time points after CLP.

Bacterial colony-forming unit determination

The peritoneal cavities were washed with 2 ml of sterile saline, and the lavage fluids were harvested. A 10 μl aliquot of lavage fluids was used to assess bacterial colony-forming units (CFU). Peritoneal fluids (PF, 10 μl) from each mouse were serially diluted with sterile saline. Each PF dilution was plated on tryptic soy blood agar plates and incubated overnight at 37°C, after which the number of aerobic colonies was counted. Data were expressed as CFU per 10 μl PF.

Cell preparation

Spleens were obtained at 24 hours after CLP from mice treated with PBS or Gal-9 immediately after CLP and dispersed into single-cell suspensions. Red blood cells (RBC) were lysed with 0.1 N NH_4Cl, and the spleen cells were washed three times with Roswell Park Memorial Institute medium (RPMI) 1640 and cultured in RPMI 1640 solution supplemented with 5% FCS, glutamine and antibiotics in a 5% CO_2 incubator for 48 hours.

Measurement of cytokines

Murine cytokines were quantitated using a standard sandwich ELISA according to the manufacturer's protocol. The capture antibodies (Abs), detection Abs and the recombinant cytokines were purchased from R&D Systems or BioLegend. The ELISAs used in this

study did not cross-react with other available murine cytokines.

Flow cytometry analysis

Spleen cells were harvested from WT and Gal-9 TG CLP mice at 24 hours after CLP, and the cells (1×10^6 cells/ml) were suspended in PBS supplemented with 2% FCS and 0.1% sodium azide. Cells were stained with mAbs specific for mouse CD3, CD4, CD8, GL-3, NK1.1 and Tim-3 (BioLegend, Tokyo, Japan). Stained cells were analyzed using a FACSCalibur (BD Biosciences, Tokyo, Japan). To assess intracellular IL-17 production, spleen cells were cultured for 48 hours in the presence of 1 μg/ml brefeldin A (Sigma, Tokyo, Japan) and were permeabilized overnight with permeabilization buffer (Cytofix/Cytoperm; eBioscience, San Diego, CA, USA).

Statistics

Statistical significance was determined using the Mann–Whitney *U*-test. In the case of survival curves, the data were analyzed using the log-rank test. A *P*-value <0.05 was regarded as statistically significant. All data were expressed as mean ± standard error of the mean (SEM).

Results and discussion

Improved survival in CLP-induced sepsis in Gal-9 TG mice

We first compared the survival rate after CLP between (WT and Gal-9 TG mice. The survival rate of Gal-9 TG mice was significantly higher than that of WT mice. Of the 19 Gal-9 TG mice, 12 survived to day 7 after CLP (63.2%), whereas only 3 of 18 WT mice survived to day 7 (16.7%) (*P* <0.01). Thus, Gal-9 TG mice were resistant to the lethality induced by CLP, thereby suggesting a beneficial effect of Gal-9 administration in mice undergoing CLP (Figure 1A).

To uncover the mechanism by which Gal-9 prolongs the survival of CLP mice, we assessed the levels of pro-inflammatory cytokines such as TNF-α and IL-1β in the PF of WT and Gal-9 TG mice at 24 hours after CLP. Figure 1B shows that the levels of TNF-α and IL-1β were relatively decreased at this time point and that the level of IL-12 was relatively increased in Gal-9 TG mice compared to WT mice. However, we previously showed that the levels of TNF-α and IL-12 in PF were significantly suppressed in Gal-9 TG mice during early periods (1 to 6 hours) of LPS-induced peritoneal inflammation [24]. In contrast, the levels of IFNγ and IL-10 were significantly decreased in Gal-9 TG mice.

We further tested whether Gal-9 could decrease the bacterial load in PF at 24 hours after CLP. The bacterial load in Gal-9 TG mice tended to be lower than the bacterial load in WT mice but the difference was not statistically significant (Figure 1C). No bacterial CFU or few bacterial CFU were found at 7 days after CLP in the PF of Gal-9-treated surviving mice, as expected (data not shown).

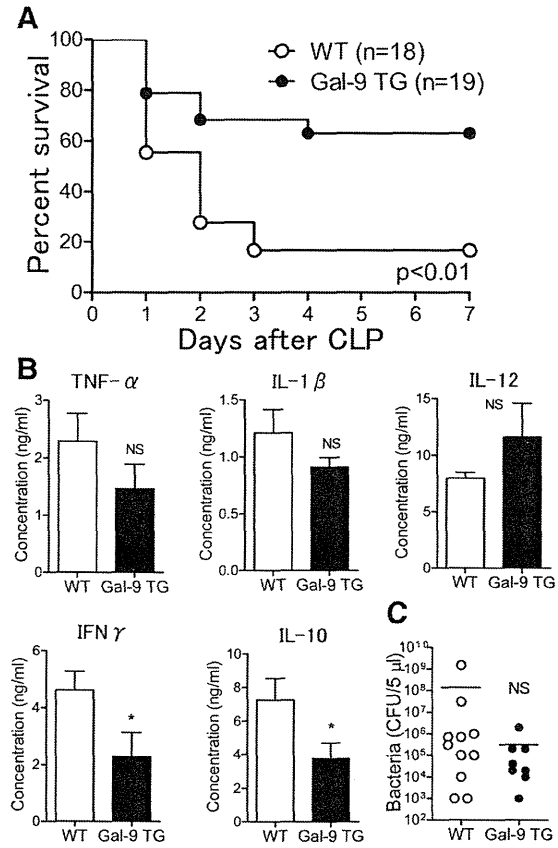

Figure 1 Survival of galectin (Gal)-9 transgenic (TG) mice during polymicrobial sepsis induced by cecal ligation and puncture (CLP). (A) Prolonged survival of Gal-9 TG mice. CLP was performed, and survival was monitored for 7 days after CLP in wild-type (WT) and Gal-9 TG CLP mice. The log-rank (Mantel-Cox) test was used for statistical analysis; *P* <0.01. **(B)** Cytokine levels in peritoneal fluids (PF) from WT (n = 18) and Gal-9 TG (n = 19) mice. At 24 hours after CLP, PF was obtained and ELISA was used for quantification of cytokine levels (**P* <0.05; NS, not significant). **(C)** Bacterial load in WT (n = 11) and Gal-9 TG (n = 8) mice. PF dilutions were plated on tryptic soy blood agar plates and incubated overnight at 37°C. The number of aerobic colonies was counted.

Delayed Gal-9 treatment prolongs the survival of CLP mice

To determine whether Gal-9 exhibits protective effects in CLP mice, we treated CLP mice with a single Gal-9 administration (intravenous (i.v.), 30 μg/mouse) immediately after CLP. As shown in Figure 2A, 7 of 16 Gal-9-treated CLP mice survived at day 7 after CLP (43.8%), whereas only 2 of 16 PBS-treated mice survived at this time point (12.5%) (*P* <0.05). We further failed to detect any significant difference in the bacterial loads of the PF between PBS- and Gal-9-treated mice at 24 hours after CLP (Figure 2B). Similar to Gal-9 TG mice, no bacterial

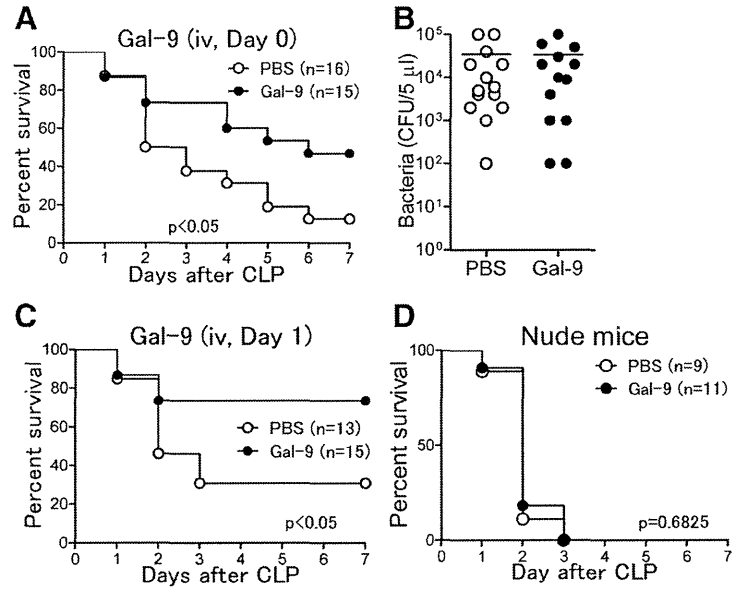

Figure 2 Delayed galectin (Gal)-9 treatment prolongs the survival of cecal ligation and puncture (CLP) mice. (A) CLP mice received a single Gal-9 injection (intravenous (i.v.), 30 μg/mouse) immediately after CLP, and survival was monitored for 7 days. The log-rank (Mantel-Cox) test was used for statistical analysis. **(B)** Bacterial load in peritoneal fluid (PF) in PBS- (n = 14) and Gal-9-treated (n = 13) mice at 24 hours after CLP. PF dilutions were plated on tryptic soy blood agar plates and incubated overnight at 37°C. The number of aerobic colonies was counted (NS, not significant). **(C)** Therapeutic effects of delayed i.v. Gal-9 injection on septic mice induced by CLP. Gal-9 was injected i.v. at 24 hours after CLP, and survival was monitored for 7 days. The log-rank (Mantel-Cox) test was used for statistical analysis; $P < 0.05$. **(D)** No therapeutic effects of i.v. Gal-9 injected immediately after CLP in nude mice. The log-rank (Mantel-Cox) test was used for statistical analysis of survival.

CFU or few bacterial CFU were found at 7 days after CLP in the PF of Gal-9-treated surviving mice (data not shown). These results suggest that direct bacterial suppression by Gal-9 is not the trigger for this prolonged survival. Further studies are required to ascertain the mechanisms how Gal-9 finally decreases bacterial CFU on Day 7.

Furthermore, delayed i.v. Gal-9 administration given at 24 hours after CLP also significantly prolonged the survival of CLP mice: 11 of 15 Gal-9-treated mice survived at day 7 after CLP (73.3%), whereas only 4 of 16 PBS-treated mice survived at this time point (25%) ($P < 0.05$) (Figure 2C). Moreover, we found that delayed subcutaneous Gal-9 treatment given at 24 hours after CLP similarly prolonged the survival of CLP mice: 15 of 22 Gal-9-treated mice survived at day 7 after CLP (68.2%), whereas 8 of 22 PBS-treated mice survived at this time point (40.0%) ($P = 0.058$). These results suggest that Gal-9 has therapeutic effects on microbial sepsis, probably by modulating the immune response to prolong the survival of CLP mice.

Interestingly, Gal-9 did not exhibit any therapeutic effects in nude mice: All animals that received Gal-9 administration died by 3 days after CLP similar to CLP mice that did not receive Gal-9 (Figure 2D), suggesting that T cells are critically involved in the survival enhancement mediated by Gal-9.

Effects of Gal-9 on plasma levels of cytokines

To determine the functions of Gal-9 in CLP mice, plasma levels of pro-inflammatory cytokines were assessed. Similar to the Gal-9 TG mice, Gal-9 failed to affect the levels of early pro-inflammatory cytokines such as TNF-α at 24 hours after CLP, although the level of IL-6 was suppressed by Gal-9 (Figure 3). In contrast, the level of HMGB1, a late inflammatory mediator [3], was markedly suppressed in Gal-9-treated mice at 24 hours after CLP (Figure 3). This result seems reasonable because delayed administration of antibodies against HMGB1 attenuates endotoxin lethality [3] and CLP-induced sepsis in rodents [4,5]. Furthermore, we found a decreased level of IL-10 and increased levels of IL-15 and IL-17 in Gal-9-treated CLP mice.

Based on the above results, we hypothesized that Gal-9 plays a critical role in not only the early but also in the late stage of sepsis, in which HMGB1 plays a critical role [27] to protect mice from lethality. This conclusion is based on our previous findings that Gal-9 administration suppresses the production